Cytological, molecular and life cycle characterization of *Anostracospora rigaudi* n. g., n. sp. and *Enterocytospora artemiae* n. g., n. sp., two new microsporidian parasites infecting gut tissues of the brine shrimp *Artemia*

NICOLAS OLIVIER RODE[1]*, JULIE LANDES[1], EVA J. P. LIEVENS[1], ELODIE FLAVEN[1]†, ADELINE SEGARD[1], ROULA JABBOUR-ZAHAB[1], YANNIS MICHALAKIS[2], PHILIP AGNEW[2], CHRISTIAN P. VIVARÈS[3,4] *and* THOMAS LENORMAND[1]

[1] *CEFE – UMR 5175, CNRS, 1919 route de Mende, 34293 Montpellier cedex 5, France*
[2] *MIVEGEC – UMR 5290, CNRS-IRD-UM1-UM2, IRD, 911 Avenue Agropolis, B.P. 64501, 34394 Montpellier Cedex 5, France*
[3] *Clermont Université, Université Blaise Pascal, Laboratoire Microorganismes: Génome et Environnement, BP 10448, F-63000 Clermont-Ferrand, France*
[4] *LMGE – UMR 6023, CNRS, F-63177 Aubière, France*

(*Received 25 January 2013; revised 10 April 2013; accepted 15 April 2013*)

SUMMARY

Two new microsporidia, *Anostracospora rigaudi* n. g., n. sp., and *Enterocytospora artemiae* n. g., n. sp. infecting the intestinal epithelium of *Artemia parthenogenetica* Bowen and Sterling, 1978 and *Artemia franciscana* Kellogg, 1906 in southern France are described. Molecular analyses revealed the two species belong to a clade of microsporidian parasites that preferentially infect the intestinal epithelium of insect and crustacean hosts. These parasites are morphologically distinguishable from other gut microsporidia infecting *Artemia*. All life cycle stages have isolated nuclei. Fixed spores measure $1{\cdot}3 \times 0{\cdot}7\,\mu$m with 5–6 polar tube coils for *A. rigaudi* and $1{\cdot}2 \times 0{\cdot}9\,\mu$m with 4 polar tube coils for *E. artemiae*. Transmission of both species is horizontal, most likely through the ingestion of spores released with the faeces of infected hosts. The minute size of these species, together with their intestinal localization, makes their detection and identification difficult. We developed two species-specific molecular markers allowing each type of infection to be detected within 3–6 days post-inoculation. Using these markers, we show that the prevalence of these microsporidia ranges from 20% to 75% in natural populations. Hence, this study illustrates the usefulness of molecular approaches to study prevalent, but cryptic, infections involving microsporidian parasites of gut tissues.

Key words: *Artemia franciscana*, *Artemia parthenogenetica*, horizontal transmission, Microsporidia, phylogeny, ultrastructure.

INTRODUCTION

The microsporidia are obligate endocellular parasites related to fungi (Thomarat *et al*. 2004; Vossbrinck *et al*. 2004) which infect most animal taxa, and some protists (Canning and Vávra, 2000). They can reach high prevalence in farm animals and in aquaculture (Weiss, 2005) and are frequently found causing opportunistic infections in immunocompromised humans (e.g. Molina *et al*. 1993). In consequence, their study is of economic, veterinary and medical importance (Texier *et al*. 2010). In addition, microsporidian infections can have strong detrimental effects on the fitness of their hosts (e.g. Stirnadel and Ebert, 1997; Otti and Schmid-Hempel, 2008; Ryan and Kohler, 2010). Hence, they can have a major impact on the demography of natural populations (Ebert *et al*. 2000).

Microsporidia are frequently found infecting natural populations of the brine shrimp *Artemia* (Codreanu, 1957), where they can alter biomass production (Martinez *et al*. 1989, 1992). However, these parasites can be difficult to study due to their small size, and only a few species infecting *Artemia* spp. have been characterized (Ovcharenko and Wita, 2005). In this paper, we combine phylogenetic, microscopic and experimental approaches to characterize two ecologically important microsporidian species (Rode *et al*. 2013). Both species cause infections which are localized in the intestinal epithelium, are small, and hence difficult to detect. To overcome this problem of detection, we developed species-specific molecular markers that allow infections to be detected within 3–6 days post-infection.

* Corresponding author. CEFE – UMR 5175, 1919 route de Mende, 34293 Montpellier cedex 5, France. E-mail: nicolas.rode@ens-lyon.org
† Present address: Institut des Sciences de l'Evolution (UM2-CNRS), Université Montpellier 2, Montpellier, France

doi:10.1017/S0031182013000668

Table 1. Description of species-specific (Msp1p2f/Msp1p3r and Msp2p1f/Msp2p3r) and universal (734F/1537R) primers used to amplify partial SSU rDNA regions from the *Msp1* and *Msp2* microsporidian parasites

Primer name	Microsporidian species	Primer sequence (5′–3′)	Product length	Tm (°C)
Msp1p2f	*Msp1*	GAAAATGTGGCTAAGGGCGC		60 °C
Msp1p3r	*Msp1*	TTTGCCAAGCATTCATCCTC	218 bp	60 °C
Msp2p1f	*Msp2*	GCGATGATTTGCTCTTGATG		60 °C
Msp2p3r	*Msp2*	AGCACTTGTTTACTGTGCCC	264 bp	60 °C
734F	*Msp1*/*Msp2*	GAAAATTAAAGAAATTGACGGA		60 °C
1537R[a]	*Msp1*/*Msp2*	TTATGATCCTGCTAATGGTTC	~ 520/530 bp[b]	60 °C

[a] Vossbrinck *et al*. (1993).
[b] The length of the sequences amplified with the 734F/1537R primers varied between *Msp1* (~ 520 pb) and *Msp2* (~ 530 bp).

We did not detect macroscopic signs of infection by these parasites, in contrast to other species where 'white-spots' visible to the naked eye often indicate the presence of a microsporidian infection (e.g. Codreanu, 1957; Martinez *et al*. 1994). Finally, we demonstrate that both species have a direct life cycle with horizontal transmission between hosts and that they are likely to be specific to the genus *Artemia*. This study shows that molecular methods are particularly useful to detect and discriminate between cryptic parasites that can remain unnoticed with microscopic techniques, despite being highly prevalent in host populations.

MATERIALS AND METHODS

Molecular detection and characterization

To investigate microsporidiosis, we sampled 133 *Artemia parthenogenetica* Bowen and Sterling, 1978 and 147 *Artemia franciscana* Kellogg, 1906 in different salterns around Aigues-Mortes (Southern France) during the summer and winter of 2008. Adult specimens were preserved in 96% ethanol and dried in 96-well plates at 56 °C. DNA was extracted using Sigma Extraction Solution (Sigma, Germany; extraction in 30 μL at 95 °C for 10 min, 20 °C for 10 min, product diluted with 50 μL of sterile deionized water). We screened for microsporidian infection using PCR with microsporidian-specific small subunit (SSU) ribosomal DNA primers (V1f/530r, Baker *et al*. 1994; Weiss *et al*. 1994). PCR amplifications were carried out in a total volume of 20 μL containing 2 μL of 10X PCR buffer (Eurogentec), 0·5 μM of each primer, 1·8 mM $MgCl_2$, 1 mM dNTPs (Eurogentec), 1 U of RedGoldStar® Taq polymerase (Eurogentec) and 1 μL of DNA extract. A negative control (PCR mix alone) was included on each extraction plate. The thermal profile consisted of a 2 min initial stage at 94 °C, followed by 35 cycles at 94 °C for 30 s, 60 °C for 1 min, and 72 °C for 2 min, with a final extension at 72 °C for 5 min. 5 μL of the PCR product was separated by electrophoresis on a 2% agarose gel containing 0·5 lg mL^{-1} GelRed™ (Biotium, USA) and visualized under UV light. The quality of the DNA template was checked by an additional PCR on all samples using host microsatellite primers (Apdq02TAIL/EU888845, Af-B10/EU 888838, Muñoz *et al*. 2008); negative samples were excluded from analysis. 67 positive PCR products were sequenced using an ABI prism 3130xl genetic analyser with an ABI Prism Big Dye Terminator Kit (Applied Biosystems, Warrington, UK). Approximately 340 bp of SSU rDNA sequence was generated for each parasite isolate; from these we detected two divergent sequences identified as *Microsporidium 1* and *2* (hereafter *Msp1* and *Msp2*). Each microsporidian sequence was found in both *Artemia* host species. Species-specific primer sets were designed to amplify the *Msp1* and *Msp2* sequences (Msp1p2f/Msp1p3r and Msp2p1f/Msp2p3r respectively, Table 1).

Phylogenetic analyses

To investigate *Msp1* and *Msp2* phylogeny, we sequenced an additional, larger fragment (~ 1250 bp) of the SSU rRNA using nested PCRs. We first amplified a fragment with the V1F/1537R primers (Vossbrinck *et al*. 1993) in two *Msp1*-infected individuals and one *Msp2*-infected individual. We subsequently amplified nested fragments with the V1F/HG4R primers (Vossbrinck *et al*. 1993; Gatehouse and Malone, 1998) and the 734F/1537R primers (Table 1). Sequences were blasted against GenBank sequences. To construct the tree, we selected the closest matches consisting of characterized microsporidian sequences (Vossbrinck and Debrunner-Vossbrinck, 2005; Wang *et al*. 2005; Tourtip *et al*. 2009; Stentiford *et al*. 2010, 2011), and also used *Msp2* sequences from Israel and the USA, which were found in a phylogeographic study of *Msp1* and *Msp2* (Rode *et al*. submitted). All sequences are given in Table S1 – in Online

version only. *Thelohania parastaci* was used as an outgroup. Sequences were aligned using the ClustalW algorithm in BioEdit v7.0.9 (http://www.mbio.ncsu.edu/bioedit/bioedit.html). To objectively remove ambiguously aligned regions, the online version of the program Gblocks (Castresana, 2000, www.phylogeny.fr) was first applied to the full dataset, allowing small final blocks and relaxed flanking regions (final length ~342 bp). A more stringent option (i.e. allowing large final blocks and strict flanking regions) was also used to analyse a restricted dataset including only sequences longer than 1 kb (excluding the following sequences: *Hepatospora* spp., *Enterospora canceri*, *Enterocytozoon hepatopenaei* and *Myospora metanephrops*, final length ~720 bp). We determined the best model for the base frequencies and substitution rates based on AICc using jModelTest 2.1.1 (TrN model with a gamma variation of mutation rate across sites, and including a fitted proportion of invariable sites for the complete dataset; Guindon and Gascuel, 2003; Darriba *et al*. 2012). Maximum likelihood analyses were carried out using Phyml v3.0 (Guindon *et al*. 2010) and the robustness of nodes was assessed with 100 bootstrap replications. Mean pairwise genetic distances between *Msp1/Msp2* and their related monophyletic clades (for which several sequences were available) were calculated using Mega 5 (Tamura *et al*. 2011) using the Kimura 2-parameter model with gamma variation across sites. Sequences of the newly characterized lineages (*Msp1*: JX915758, JX915759; *Msp2*: JX915760) have been deposited in GenBank.

Light and transmission electron microscopy

To characterize the two microsporidian species, we established laboratory cultures infected either with *Msp1* or *Msp2*, using wild-caught samples. As both *Msp1* and *Msp2* cannot be vertically transmitted through cysts (Rode *et al*. in press), we established uninfected laboratory cultures with nauplii hatched from cysts isolated from two populations (Site 9, 2010, N43°32′25″-E4°13′26″, Pont l'Abbé, 2011, N43°32′40″-E4°9′17). Three *A. parthenogenetica* females infected with *Msp1* and three *A. franciscana* females infected with *Msp2* were used for microscopy analyses. Two *A. parthenogenetica* and two *A. franciscana* females from uninfected cultures were used as negative controls. Each female was cut in half; the anterior part was PCR-tested to confirm infection status and the posterior part was fixed in 2·5% glutaraldehyde in Sorensen's buffer (0·1 M, pH 7·4) and kept overnight at 4 °C. Specimens were washed in Sorensen's buffer and post-fixed in the dark for 2 h, in 0·5% osmium tetroxide at room temperature. After washing in three changes of Sorensen's buffer, the specimens were dehydrated in a graded ethanol series (30–100%) before being embedded in EMbed-812 (Electron Microscopy Sciences, Fort Washington, USA) using an Automated Microwave Tissue Processor for Electronic Microscopy (Leica EM AMW, Bensheim, Germany). Semi-thin (1 μm) and ultra-thin sections (70 nm, Leica-Reichert Ultracut E) were collected at different levels of each block. Semi-thin sections were stained with toluidine blue to identify suitable target areas with a light microscope. Ultra-thin sections of these areas were mounted on uncoated copper grids and counterstained with uranyl acetate and subsequently observed using a Hitachi 7100 transmission electron microscope (TEM) at the Centre de Ressources en Imagerie Cellulaire (CRIC, Montpellier, France). We examined different tissues (hypoderm, musculature, intestinal epithelium, ovaries), as well as the haemocoel of each infected individual. Measurements were made using the on-board calibrated measuring software of the TEM.

Transmission mode and life cycle of Msp1 *and* Msp2

A complete and rational classification of microsporidia requires that the description of new species includes information on their life cycle and transmission behaviour (Becnel, 1992). These characteristics are also important for our understanding of the ecology and evolution of this group. First, in order to test for horizontal transmission of infection between hosts, we placed ~20 individuals from uninfected cultures in 10-L tanks containing a mix of *A. franciscana* individuals from cultures infected either by *Msp1* or *Msp2* (replicated three times). Hence, transmission could occur through the ingestion of spores released from the decomposing tissues of dead hosts and/or from spores released with the faeces of living hosts. After 3 weeks, five *A. parthenogenetica* individuals from each tank were randomly selected and PCR-tested. Second, in order to test for vertical transmission of infection to *Artemia* spp. nauplii, we isolated cultured *A. parthenogenetica* females of known infection status ($n(Msp1)=6$), $n(Msp2)=6$) and wild-caught *A. parthenogenetica* ($n=4$) and *A. franciscana* ($n=9$) females of unknown infection status. All females were maintained individually (*A. parthenogenetica* females) or with males (*A. franciscana* females) in 300 mL jars filled with 50 g L^{-1} artificial seawater (Instant Ocean, Aquarium Systems, Mentor, Ohio). To prevent horizontal transmission, jars were checked twice daily and any newborn nauplii were immediately transferred to new medium, after which the female was killed and preserved in 96% ethanol. 220 nauplii were recovered. To maximize the chance of detecting microsporidian infection, PCR tests were performed on pools of 3 to 5 sibling individuals of different ages (mean = 16·4 d, min = 0 d, max = 38 d).

In order to investigate the possibility that these parasites infect other hosts co-occurring with

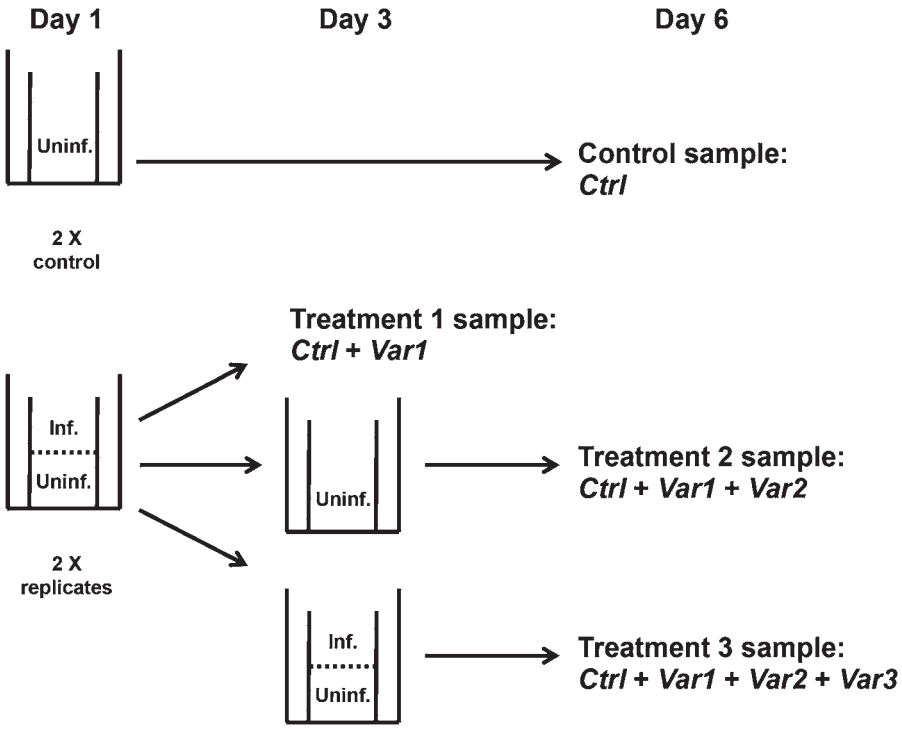

Fig. 1. Timing of *Msp1* and *Msp2* detection by PCR. In the control, individuals were kept isolated in the absence of infected donors (Control). For all other treatments, recipient hosts (Uninf.) were placed underneath infected hosts (Inf.) for 2 days. After these 2 days, 25% of the recipient hosts were killed and conserved in ethanol (Treatment 1), 25% were kept isolated in the absence of infected donors for 4 additional days (Treatment 2), and the remaining 50% were kept with infected donors for 4 additional days (Treatment 3). Detection time was investigated by comparing the reference control (*Ctrl*) to three indicator variables (*Var1*: Exposure and incubation Day 1–2, *Var2*: Incubation Day 3–6, *Var3*: Exposure Day 3–6). All treatments were replicated twice.

Artemia in the Aigues-Mortes salterns, we used PCR to test for the presence of infection in heterotrichous cilitates ($n=20$), harpacticoida copepods ($n=6$) and *Potamonectes cerisyi* beetles ($n=2$). Host DNA quality was checked using universal primers for the COI mitochondrial gene (LCO1490/HCO2198, Folmer *et al*. 1994).

Visible signs of infection

Artemia often exhibit 'white-spots' upon microsporidian infection (Codreanu, 1957; Martinez *et al*. 1992, 1994). Since *Artemia* in Aigues-Mortes exhibit such white-spots on their cuticle or in the posterior part of their digestive tracts, we investigated association of these symptoms with *Msp1* and/or *Msp2* infection. We sampled *A. parthenogenetica* and *A. franciscana* individuals ($n=1243$) in three salterns in Aigues-Mortes in May 2011 and recorded the presence of white-spots on the cuticle and in the digestive tract using a stereomicroscope. Upon observation, individuals were killed and placed in ethanol in 96-well plates and PCR-tested for *Msp1* and *Msp2* infection using the aforementioned species-specific primers. We analysed the presence of white-spots on the cuticle and digestive tract separately using generalized linear models with a Bernoulli distribution (package 'stats' in R 2.14.2). We tested the influence of *Msp1* and *Msp2* infection, host species and their interactions using likelihood ratio tests.

Timing of Msp1 *and* Msp2 *detection by PCR*

To measure the latency of PCR detection after infection, we placed 20 *A. parthenogenetica* and 20 *A. franciscana* uninfected recipient individuals in contact with 30 *Msp1*-, 30 *Msp2*-infected and 20 co-infected donor individuals. To get an average latency across different host genetic backgrounds, we used recipient hosts from different populations (*A. franciscana* and *A. parthenogenetica*: Aigues-Mortes, France, *A. parthenogenetica*: LaMata, Spain. *A. franciscana*: San Francisco Bay, CA, USA). Donors were kept above recipients in the water column using a tank with two compartments separated by nylon mesh (0·2 mm), which allowed microsporidian spore contamination, but prevented donor and recipient hosts from mixing. After 2 days, half of the recipients were killed and placed in ethanol (Treatment 1, Exposure and Incubation Day 1–2, Fig. 1). The remaining recipients were placed in new medium in the absence of donors for another 4 days (Treatment 2, Exposure and Incubation Day 1–2 + Incubation Day 3–6, Fig. 1). We also placed uninfected individuals in similar tanks for

6 continuous days, in the presence (Treatment 3, Exposure and Incubation Day 1–2 + Incubation Day 3–6 + Exposure Day 3–6, Fig. 1) or absence (Control) of infected donor individuals ($n = 20$ and 10, respectively). Treatments and controls were replicated twice. All recipient individuals were PCR-tested for infection by *Msp1* or *Msp2* using the above-mentioned species-specific primers. We analysed the probability of detection using generalized linear models with a binomial distribution (package 'Stats' in R 2.14.2). More specifically, we introduced three indicator variables nested within treatments: Exposure and Incubation Day 1–2, Incubation Day 3–6, Exposure Day 3–6, which reflect the increasing chance of infection in the control, treatment 1, treatment 2 and treatment 3. We tested whether each of these variables was significantly different from zero using likelihood ratio tests and we checked for overdispersion in the best model.

RESULTS

Detection and prevalence

As explained above, we successfully developed primers specific to *Msp1* and *Msp2*. These primers were used to estimate the prevalence of *Msp1* and *Msp2* in the original sample (147 *A. franciscana* and 133 *A. parthenogenetica*). The two parasites were highly prevalent: 39·5% in *A. franciscana*, 75·2% in *A. parthenogenetica* for *Msp1*; 52·4% in *A. franciscana*, 21·8% in *A. parthenogenetica* for *Msp2*.

Phylogeny

We recovered 1211 and 1238 bp SSU fragments (excluding the V1F and 1537R primer sites) for the longest sequences of *Msp1* and *Msp2*, respectively. The phylogenetic reconstruction based on all well-known related taxa indicated that: (1) *Msp1* and *Msp2* were included in a microsporidian clade comprised of species infecting mostly the intestinal epithelium of insect and crustacean hosts (Fig. 2). (2) *Msp1* belonged to a group including well-known species from the *Endoreticulatus* and *Cytosporogenes* genera known to mainly infect the gut epithelium of insects (Group 1, Fig. 2). *Msp1* divergence with these two genera was low (average divergence of 3·5% with *Endoreticulatus* species and 6·6% with *Cytosporogenes* species, Table S2 – in Online version only). Molecular divergence with other species from this group was similar ($\sim$ 6·0%, Table S2). (3) *Msp2* was closely related to a first group, which included the genera *Endoreticulatus* and *Cytosporogenes* along with *Msp1*, and to a second group including different genera: *Nucleospora, Paranucleospora, Desmozoon, Enterocytozoon, Enterospora, Hepatospora* (Group 1 and Group 2, respectively, Fig. 2). *Msp2* was twice as divergent from Group 2 as from Group 1 (22·5 and 11·7% respectively, Table S3 – in Online version only), which was likely due to a higher rate of molecular evolution within Group 2 (Fig. 2). (4) The exclusion of short sequences revealed that Group 1, 2 and *Msp2* were a sister group to Group 3 including *Orthosomella* and *Libermannia* species (Fig. S1 – in Online version only). The latter species were on average more divergent from Group 1 and Group 2 than from *Msp2* (18·5, 21·9 and 14·5% respectively, Table S3). Overall, phylogenetic positions were qualitatively similar when excluding shorter sequences (Fig. S1).

Light and transmission electron microscopy study of Msp1 (Anostracospora rigaudi *n. g., n. sp.*)

The results from the light and TEM microscopy are summarized in Table S4 – in Online version only. Semi-thin sections of *Msp1*-infected individuals (as checked by PCR) were examined for tissue infection using light microscopy. *Msp1* infections were restricted to enterocytes. Parasitophorous vacuoles filled the space between the nucleus and the brush border (Fig. 3A). The number of mature spores in parasitophorous vacuoles estimated from sections ranged between 32 and 64 (Fig. 3B and C). Enterocytes with parasitophorous vacuoles were released in the intestinal lumen (Fig. 3D). Free parasitophorous vacuoles including immature and mature spores were also shed in the intestinal lumen (Fig. 3E). *Msp1*-infected cells were not hypertrophied. TEM observations confirmed the localization of *Msp1* in the intestinal epithelium. The earliest stages observed were unikaryotic ribosome-rich meronts delimited by a single cytoplasmic membrane (Fig. 4A). Initial merogony did not involve a parasitophorous vacuole and occurred in direct contact with host cell cytoplasm (Fig. 4A). Merogonial divisions could not be observed, but likely occurred by plasmotomy of a merogonial plasmodium (Fig. 4B). The number of successive merogonial divisions could not be determined. Sporogony started with the development of a spore wall primordium that progressively thickened (Fig. 4C and D). Sporonts were also unikaryotic (Fig. 4B and D). They developed within a parasitophorous vacuole (Fig. 4D), sometimes together with meronts (Fig. 4B). Sporoblasts were likely to divide by plasmotomy of a sporogonial plasmodium, as suggested by the constriction in Fig. 4E. Sporoblast maturation involved an increased ribosome concentration resulting in electron-dense late sporoblasts (Fig. 5A–C). Sporoblasts with a developing invasion apparatus were sometimes observed together with mature spores in the same parasitophorous vacuole (Fig. 5A). Spores were unikaryotic and oval; their size was small: $1{\cdot}3 \times 0{\cdot}7\ \mu$m. The *Msp1* polaroplast comprised an external lamellar part (Fig. 5D and F) and an internal vesicular part

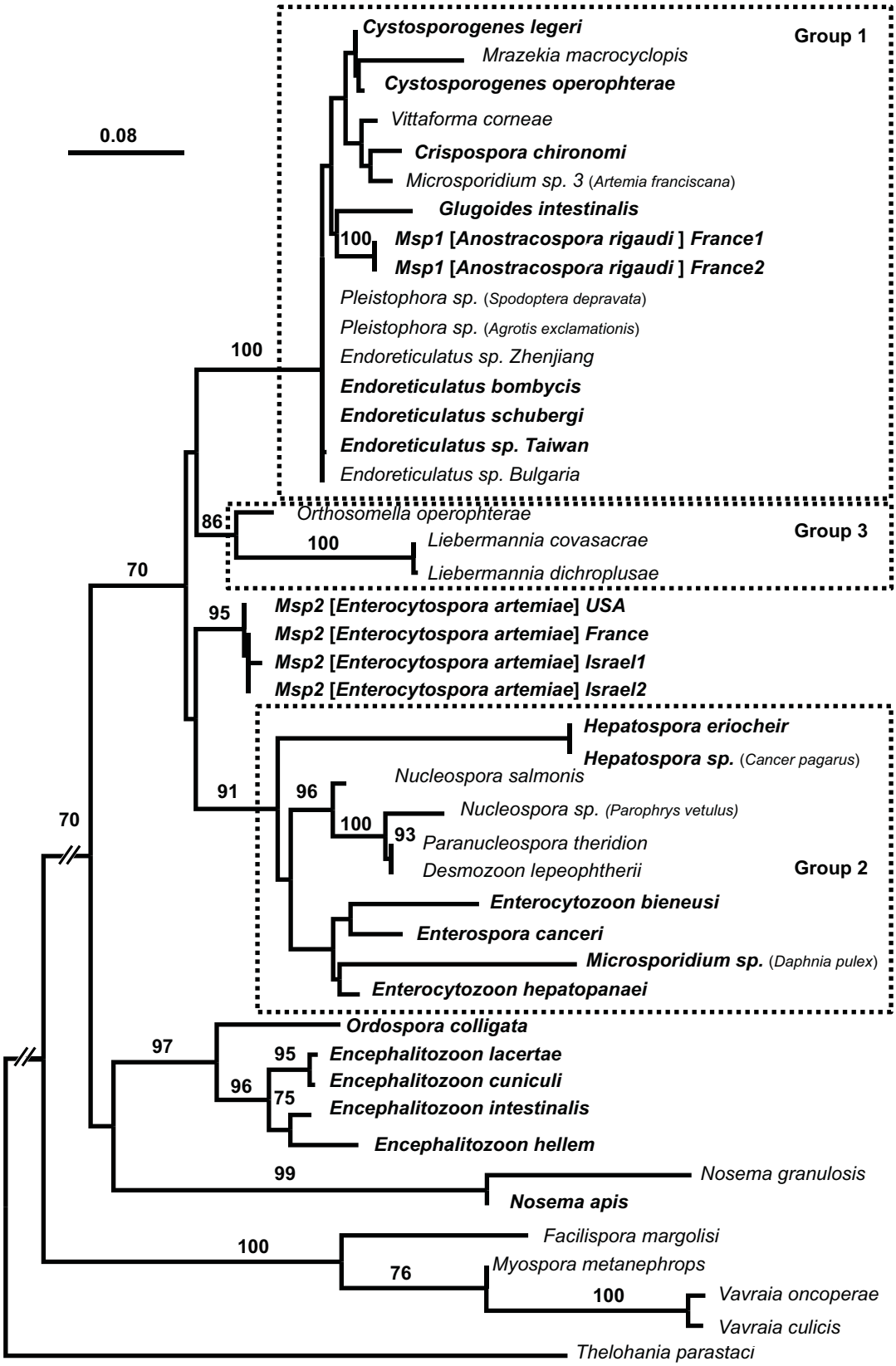

Fig. 2. Maximum likelihood tree of the SSU rDNA of *Msp1* and *Msp2* along with related microsporidian species infecting crustacean and non-crustacean hosts. Names of species infecting the digestive tract epithelium appear in bold. The host species of undescribed microsporidia appear between parentheses. Numbers above branches indicate bootstrap supports from 100 resamplings (only values above 70 are reported). Bootstrap supports for the two nodes showing *Msp2* as a sister species to Group 2 and Group 3 as a sister taxa to Group 1 were very low (32% and 36% respectively).

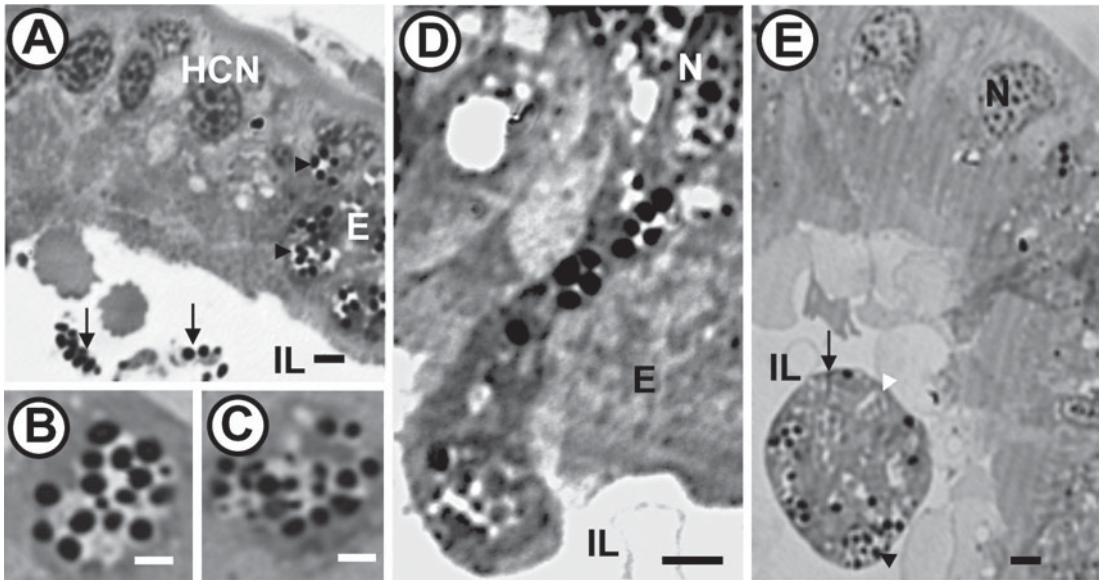

Fig. 3. Light micrographs of semi-thin sections showing *Msp1* (*Anostracospora rigaudi* n. g., n. sp.) infecting the intestinal epithelium of *Artemia parthenogenetica*. (A) Parasitophorous vacuoles (arrowheads) within an enterocyte (E) containing immature and mature spores. Release of parasitophorous vacuoles (arrows) into the intestinal lumen (IL). Scale bar = 2·5 μm. (B and C) Parasitophorous vacuoles with sporoblasts and mature spores. Scale bar = 2 μm. (D) Enterocyte containing a parasitophorous vacuole being shed into the intestinal lumen (IL). N: nucleus. Scale bar = 3 μm. (E) Parasitophorous vacuole (arrow) released into the intestinal lumen (IL), containing both early (white arrowhead) and late (black arrowhead) microsporidian stages. N: nucleus. Scale bar = 2·5 μm.

(Fig. 5G). Spore walls had a reduced thickness (55 nm, Fig. 5D, E and G) and consisted of an internal, electron-lucent chitinous endospore (40 nm) and a thinner external electron-opaque exospore (15 nm). Spore wall thickness was reduced to 25 nm at the apex of the spore (Fig. 5F and G). The polar tube (60-nm diameter) was isofilar with five or six coils aligned in one or two rows (Fig. 5C and E).

Light and transmission electron microscopy study of Msp2 (Enterocytospora artemiae *n. g., n. sp.*)

Semi-thin sections of *Msp2*-infected individuals (as checked by PCR) were examined for tissue infection using light microscopy. *Msp2* infections were restricted to enterocytes. Parasitophorous vacuoles filled the space between the nucleus and the brush border (Fig. 6A).

The number of immature and mature spores in parasitophorous vacuoles estimated from sections ranged between 64 and 128 (Fig. 6B, D and E). Enterocytes with parasitophorous vacuoles were released in the intestinal lumen (Fig. 6D). Free parasitophorous vacuoles were also observed in the intestinal lumen (Fig. 6E). TEM observations confirmed the localization of *Msp2* in the intestinal epithelium. The earliest stages observed were unikaryotic ribosome-rich meronts delimited by a single cytoplasmic membrane (Fig. 7A) and included in a parasitophorous vacuole (Fig. 7A and B). Merogonial divisions occurred by binary fission, as suggested by the occurrence of meronts with only two nuclei (Fig. 7C). The number of merogonial divisions could not be estimated. Sporonts and further developmental stages were found within a parasitophorous vacuole (Fig. 7D and E). Sporogonial division occurred by plasmotomy (Fig. 7D). Sporoblasts were found in the same vacuole as meronts and sporonts, showing an important delay in the developmental cycle (Fig. 8A), while mature spores were found in the same vacuole as late sporoblasts (Fig. 8D). Sporoblasts were uninucleate and appeared darker than meronts (Fig. 8A and B). Sporoblast maturation was characterized by the development of the invasion apparatus including the anchoring disc and the polar tube (Fig. 8B and E). The polar tube comprised a straight anterior part (manubrium) and a rolled posterior part (Fig. 8E). The polaroplast developed secondarily in late sporoblasts (Fig. 8D, F and G). Spores were unikaryotic, subspherical and small (1·2 × 0·9 μm). Spore walls were 80 nm thick (Fig. 8H and I) and consisted of an external electron-dense exospore (15 nm) and an internal electron-lucent chitinous endospore (65 nm). Spore wall thickness was reduced to 45 nm at the apex of the spore (Fig. 8H). The polar tube (100 nm diameter) was isofilar with four coils aligned in one row (Fig. 8F). The polaroplast comprised an internal lamellar part (Fig. 8H and I) and a very large external vesicular part (Fig. 8H and I; the low resolution of the polaroplast structures might be due to the low concentration of osmium tetroxide used for the post-fixation).

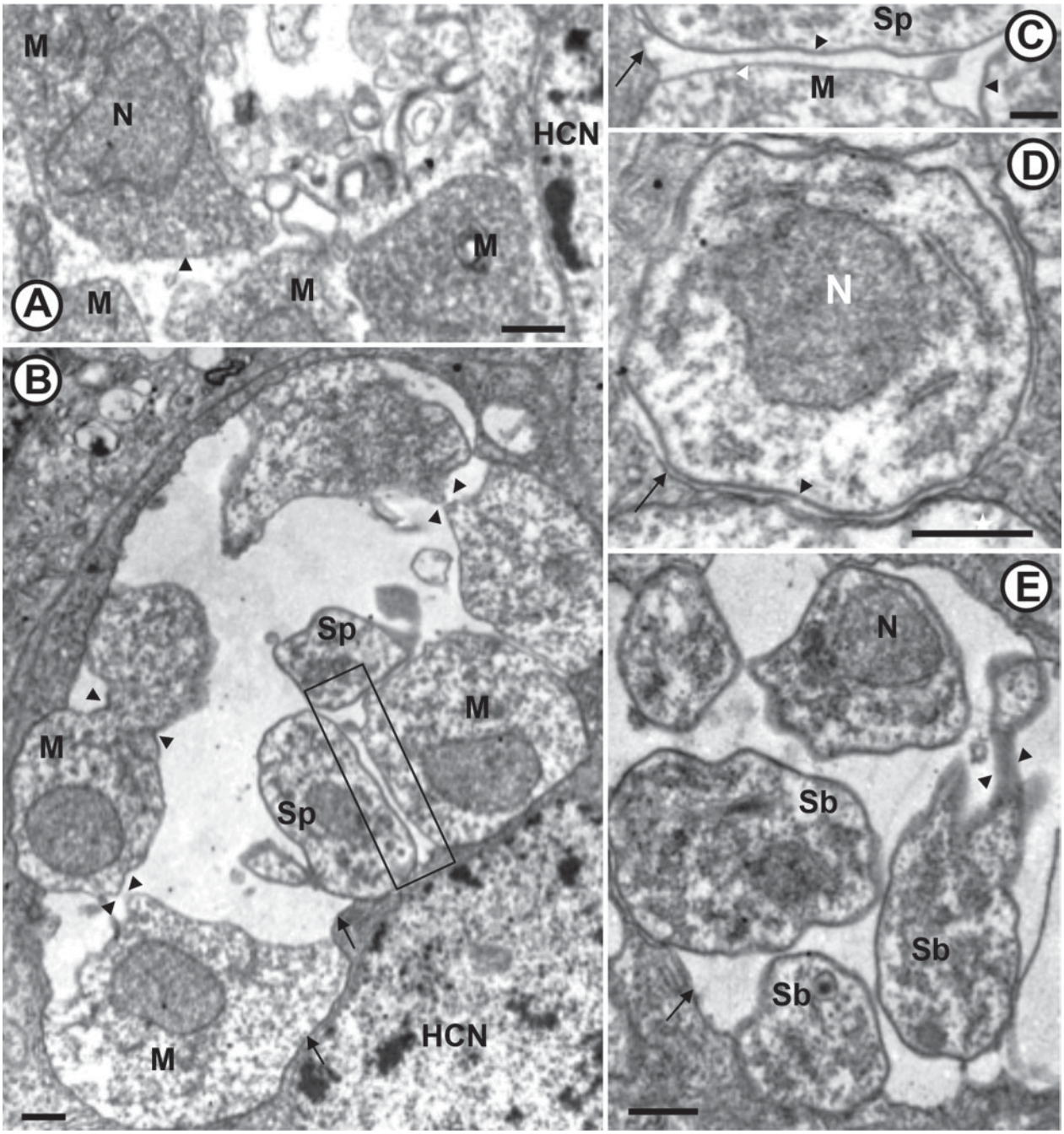

Fig. 4. Transmission electron micrographs of *Msp1* (*Anostracospora rigaudi* n. g., n. sp.) infecting the intestinal epithelium of *Artemia parthenogenetica*. (A) Four uninucleate meronts (M) limited by a cytoplasmic membrane (arrowhead) in direct contact with host cell cytoplasm. N: nucleus; HCN: host cell nucleus. Scale bar = 500 nm. (B) Parasitophorous vacuole (arrows) filled with meronts (M) and sporonts (Sp) (the former likely resulting from merogonial division by plasmotomy, arrowheads). HCN: host cell nucleus. Scale bar = 500 nm. An enlargement of the rectangular area is shown on micrograph C. (C) Membrane of the parasitophorous vacuole (arrow), meront (M) cytoplasmic membrane (white arrowhead) and sporont (Sp) cytoplasmic membrane coated with a thick sporont wall (black arrowhead). Scale bar = 200 nm. (D) Uninucleate sporont with a thick membrane (black arrowhead) within a parasitophorous vacuole (arrow). Scale bar = 500 nm. (E) Early uninucleate sporoblasts (Sb) likely resulting from sporogonial division by plasmotomy (arrowhead) within a parasitophorous vacuole (arrow). N: nucleus. Scale bar = 500 nm.

Transmission mode and life cycle of Msp1 *and* Msp2

Three weeks after their introduction into the tanks containing *Msp1*- or *Msp2*-infected *A. franciscana* individuals, the prevalence of infection in *A. parthenogenetica* hosts was 100 and 70% respectively ($n = 5$ individuals tested per tank). Hence, horizontal transmission seemed to be efficient for both *Msp1* and *Msp2*. Transmission probably resulted from filter-feeding of spores released in the

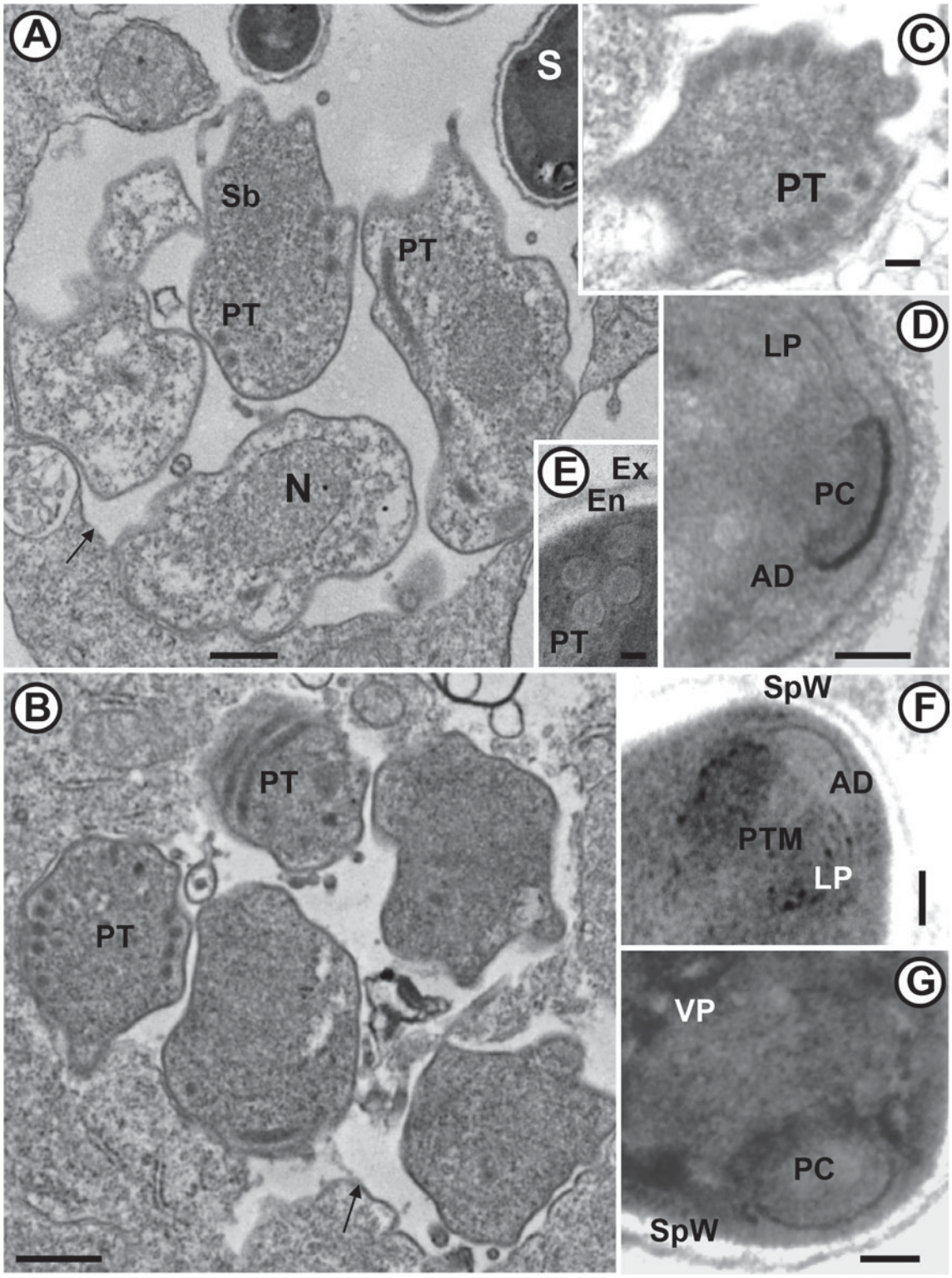

Fig. 5. Transmission electron micrographs of *Msp1* (*Anostracospora rigaudi* n. g., n. sp.) infecting the intestinal epithelium of *Artemia parthenogenetica*. (A) Uninucleate sporoblasts (Sb) with a developing polar tube (PT) together with mature spores (S) within a parasitophorous vacuole (arrow). N: nucleus. Scale bar = 500 nm. (B) Sporoblasts showing developing rolled polar tube (PT) within a parasitophorous vacuole (arrow). Scale bar = 500 nm. (C) Sporoblast showing a polar tube with 6 coils. Scale bar = 100 nm. (D) Apex of a mature spore showing the polar cap (PC), the anchoring disc (AD) and the lamellar polaroplast (LP). Scale bar = 100 nm. (E) Detail of a mature spore with 5 polar tube coils aligned in 2 rows (PT) and a spore wall comprising the thick electron-lucent chitinous endospore (En) and the thin electron-dense exospore (Ex). Scale bar = 100 nm. (F) Apex of the spore showing the spore wall (SpW), the anchoring disc (AD), the lamellar polaroplast (LP) and the manubrium of the polar tube (PTM) of a mature spore. Scale bar = 100 nm. (G) Apex of the spore showing the spore wall (SpW), the polar cap (PC) and the vesicular polaroplast (VP). Scale bar = 100 nm.

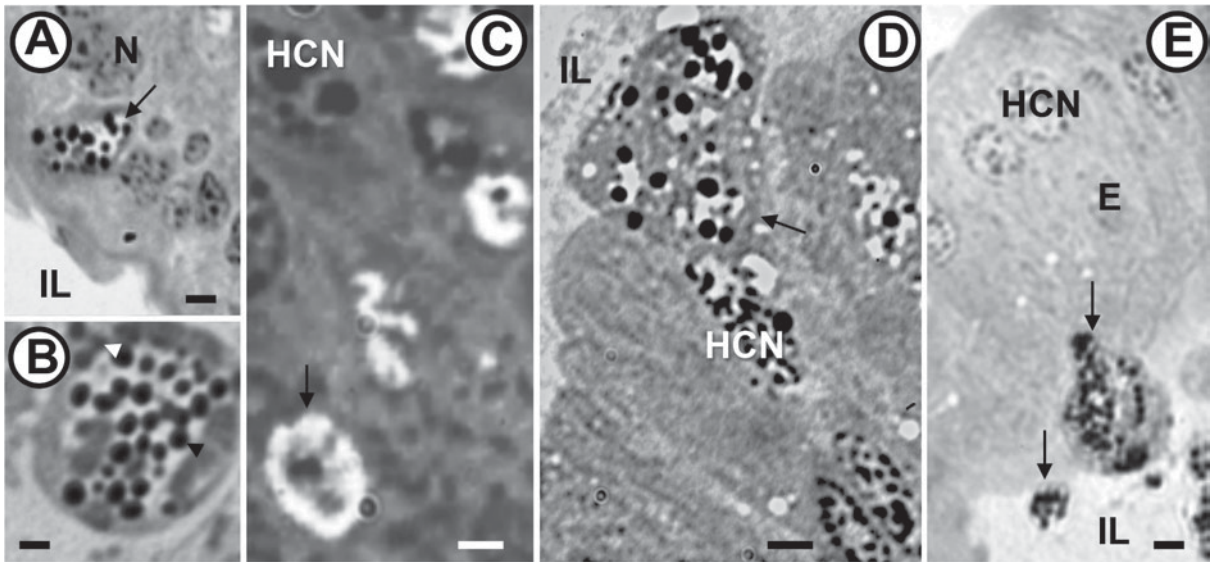

Fig. 6. Light micrographs of semi-thin sections showing *Msp2* (*Enterocytospora artemiae* n. g., n. sp.) infecting the intestinal epithelium of *Artemia franciscana*. (A) Parasitophorous vacuole (arrow) within an enterocyte. N: Nucleus; IL: intestinal lumen. Scale bar = 3 μm. (B) Parasitophorous vacuole with immature (white arrowhead) and mature (black arrowhead) spores. Scale bar = 2 μm. (C) Parasitophorous vacuole (arrow) containing a parasite stage with two nuclei. HCN: host cell nucleus. Scale bar = 2 μm. (D) Parasitophorous vacuole (arrow) containing mainly mature spores (estimated as up to 55 in sections) shed into the intestinal lumen (IL). HCN: host cell nucleus. Scale bar = 3 μm. (E) Parasitophorous vacuoles (arrow) released together into the intestinal lumen (IL). E: enterocyte; HCN: host cell nucleus. Scale bar = 2·5 μm.

faeces of infected hosts, as in related microsporidia (Ebert *et al*. 2000).

We examined the progeny of 25 potentially infected females to investigate whether they would transmit infection vertically. *A posteriori* verification of their infection status revealed that 5 *A. parthenogenetica* females were infected by *Msp1*, 7 *A. parthenogenetica* and 4 *A. franciscana* females were infected by *Msp2*, and 9 females (4 *A. parthenogenetica* and 5 *A. franciscana*) were not infected. No infection was found in the 32 nauplii produced by *Msp1*-infected females. Hence vertical transmission of *Msp1* to nauplii was unlikely. Regarding *Msp2*, one pool of 3 nauplii was detected as being infected, among the 128 nauplii tested. This might indicate rare vertical transmission. However, the other 7 siblings of the positive nauplii were not infected, which is at odds with the usual finding that the vertical transmission of microsporidia is correlated at the within-clutch level (e.g. Dunn and Hatcher, 1997). Furthermore, we did not see or detect any infection in the ovaries. This mode of transmission has not been described for gut microsporidia in related groups (Groups 1, 2, Fig. 2) and is inconsistent with the overall biology of the microsporidia infecting these tissues. Hence our finding is more likely to result from DNA contamination or early horizontal transmission before nauplii were isolated rather than from vertical transmission *per se*. We conclude that both microsporidian species are likely to be exclusively horizontally transmitted.

Although sample sizes were limited, we did not detect *Msp1* or *Msp2* infections in the few other species co-occurring with *Artemia* in the Aigues-Mortes salterns. Both microsporidia are therefore likely to be specific to the *Artemia* genus and to have direct life cycles.

Visible signs of infection

The presence of white-spots on the cuticle differed between *A. parthenogenetica* and *A. franciscana*, as *A. parthenogenetica* individuals were three times more likely to display white-spots ($P < 0{\cdot}01$, Table 2). However, the presence of white-spots on the cuticle did not depend on infection by either *Msp1* or *Msp2* ($P > 0{\cdot}05$, Table 2). Similarly, the presence of white-spots in the posterior part of the digestive tract was independent of host species and of infection by *Msp1* or *Msp2* ($P > 0{\cdot}05$, Table 2). Overall, there was no association between white-spots and *Msp1* or *Msp2* infection.

Timing of Msp1 *and* Msp2 *detection by PCR*

In the infection experiments, some individuals in the negative controls were found to be infected with *Msp1* (Table 3), and subsequent tests of the laboratory cultures used to supply the uninfected hosts for the experiment revealed that one *A. parthenogenetica* culture was infected with *Msp1*. However, this *Msp1*-contamination did not affect our conclusions, as the effects of the three indicator

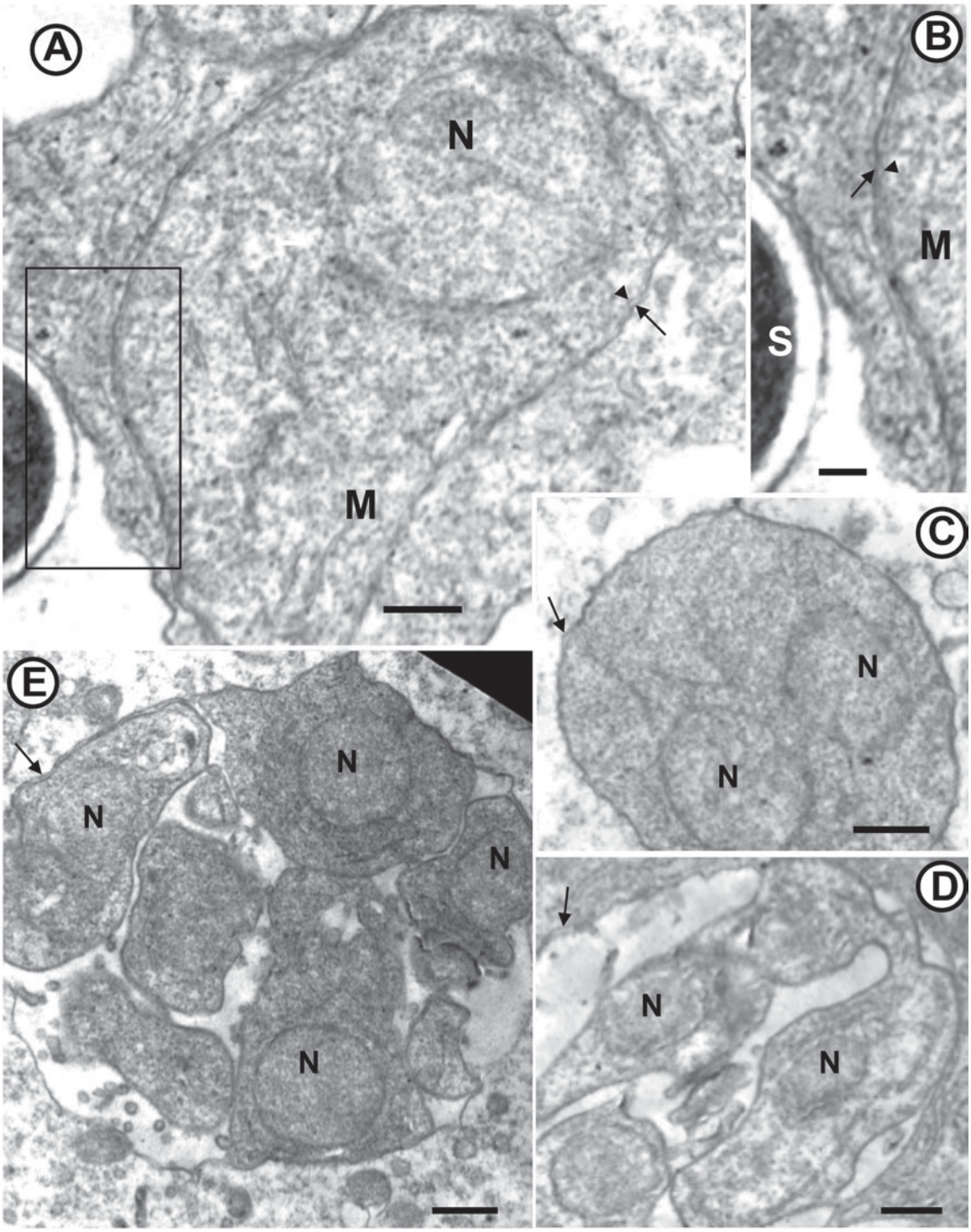

Fig. 7. Transmission electron micrographs of *Msp2* (*Enterocytospora artemiae* n. g., n. sp.) infecting the intestinal epithelium of *Artemia franciscana*. (A) Ribosome-rich uninucleate meront (N: nucleus) with a cytoplasmic membrane (arrowhead) and included within a parasitophorous vacuole (arrow). Scale bar = 500 nm. An enlargement of the rectangular area is shown on micrograph B. (B) Cytoplasmic membrane (arrowhead) of the meront (M) and parasitophorous vacuole (arrow). S: mature spore. Scale bar = 220 nm. (C) Meront with two nuclei (N), likely resulting from a binary division. Arrow: parasitophorous vacuole. Scale bar = 500 nm. (D) Chain of uninucleate sporonts resulting from the division of a sporontal plasmodium by plasmotomy. Arrow: parasitophorous vacuole; N: nucleus. Scale bar = 500 nm. (E) Parasitophorous vacuole (arrow) with uninucleate sporonts in section. N: nucleus. Scale bar = 500 nm.

variables were calculated relative to the controls. The proportion of *Msp1*- or *Msp2*-infected individuals, as detected by PCR, did not increase after 2 days of exposure to the parasite (Exposure and Incubation Day 1–2, $P > 0{\cdot}05$, Table 3). In contrast, for both *Msp1* and *Msp2*, this proportion increased strongly after the 4 days of additional incubation (Incubation Day 3–6, $P < 0{\cdot}001$, Table 3). This result

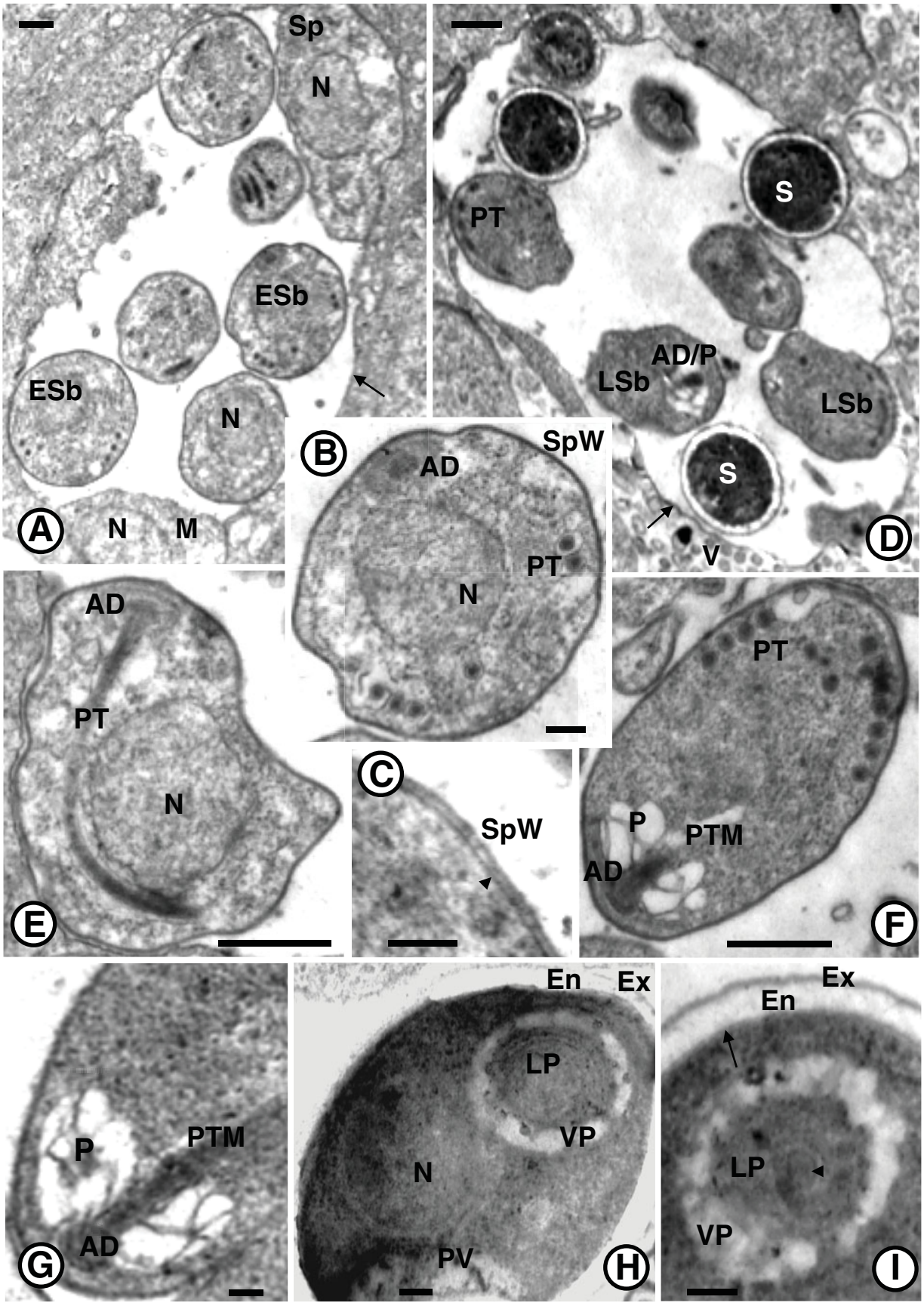

Fig. 8. Transmission electron micrographs of *Msp2* (*Enterocytospora artemiae* n. g., n. sp.) infecting the intestinal epithelium of *Artemia franciscana*. (A) Uninucleate meront (M), sporont (Sp) and early sporoblasts (ESb) within the same parasitophorous vacuole (arrow). N: nucleus. Scale bar = 500 nm. (B) Uninucleate early sporoblast with developing polar tube (PT) and anchoring disc (AD). SpW: sporont wall; N: nucleus. Scale bar = 200 nm. (C) Enlargement of the

Table 2. Analyses of the presence of white-spots on the cuticle (A) or on the posterior part of the digestive tract (B)

	$\chi^2_{(1)}$	*P-value*
A		
Host species	8·77	**
Msp1 presence	1·44	ns
Msp2 presence	0·0003	ns
B		
Host species	1·28	ns
Msp1 presence	2·98	ns
Msp2 presence	1·28	ns

** $P<0·01$.

Table 3. Analyses of *Msp1* (A) and *Msp2* (B) spore detection probability. Intercepts represent detection probability in the control (logit scale). The three variables are given relative to the intercept and were fitted using the control and the three treatments (Treatment 1: Exposure and Incubation Day 1–2, Treatment 2: Exposure and Incubation Day 1–2 + Incubation Day 3–6, Treatment 3: Exposure and Incubation Day 1–2 + Incubation Day 3–6 + Exposure Day 3–6)

	Estimate	S.E.	$\chi^2_{(1)}$	*P*-value
A				
Intercept	−0·77	0·49		
Exposure and incubation day 1–2	−0·29	0·61	0·22	ns
Incubation day 3–6	1·72	0·50	21·94	***
Exposure day 3–6	−0·04	0·42	0·01	ns
B				
Intercept	−18·57	1496·40		
Exposure and incubation day 1–2	14·93	1496·40	0·80	ns
Incubation day 3–6	2·86	1·07	30·47	***
Exposure day 3–6	0·22	0·43	0·28	ns

*** $P<0·001$.

demonstrates that *Msp1* and *Msp2* DNA is detectable by PCR between 3 and 6 days post-inoculation. Lastly, the proportion of *Msp1*- or *Msp2*-infected individuals was similar when individuals were continuously exposed to parasites throughout days 1–6 and when individuals were only exposed for days 1–2 and subsequently isolated (Exposure Day 3–6, $P>0·05$, Table 3). Two non-exclusive hypotheses could explain this result. First, infection probability could differ between individuals, all susceptible individuals being infected in the first 2 days with no subsequent infection. Second, infection could be undetectable until 5–6 days post-inoculation, with only early-infected individuals being detected in all treatments.

DISCUSSION

Phylogenetic analyses indicate that both *Msp1* and *Msp2* belong to a clade of microsporidia that mostly infect the intestinal epithelium of arthropods (insects and crustaceans). Light and ultrastructural examination of *Msp1*- and *Msp2*-infected hosts confirmed that only the gut is affected.

Comparison of Msp1 *and* Msp2 *with other microsporidia infecting* Artemia

Only two of the six known microsporidian species infecting *Artemia* spp. are gut-specific (Ovcharenko and Wita, 2005). The first species, *Unikaryon exiguum*, infects Romanian *A. parthenogenetica* and is morphologically similar to *Glugoides intestinalis* (previously named *Pleistophora intestinalis*, Codreanu, 1957). However, the size of the spores is larger in *U. exiguum* (3·2–2·6 μm) than in *Msp1* and *Msp2* (1·3–0·7 μm for *Msp1*, 1·2–0·9 μm for *Msp2*). *Unikaryon exiguum* also differs from *Msp2* as its parasitophorous vacuole appears only during merogony and its sporonts divide by binary fission (Codreanu and Codreanu-Balcescu, 1980). The second intestinal species is *Ordospora duforti* (previously named *Endoreticulatus duforti*, Martinez *et al*. 1993; Larsson *et al*. 1997), whose meronts have rosette-like division, in contrast to *Msp2* whose meronts divide by binary fission. *Ordospora duforti* also has different spore features when compared

early sporoblast in B, showing the cytoplasmic membrane (arrowhead) coated with a thick continuous sporont wall (SpW). Scale bar = 100 nm. (D) Electron-dense late sporoblasts (LSb) with developing polar tube (PT) and anterior part of the invasion apparatus (AD: anchoring disc, P: polaroplast). Parasitophorous vacuole (arrow) including late sporoblasts (LSb) and spores (S) ejected into the intestinal lumen. V: intestinal villi. Scale bar = 500 nm. (E) Early sporoblast with developing anchoring disc (AD) and polar tube (PT) around the nucleus (N). Scale bar = 500 nm. (F) Late sporoblast with a developing polar tube manubrium (PTM), anchoring disc (AD) and vesicular polaroplast (VP) at the apex. At the posterior part, 6 coils of the polar tube (PT) are aligned in one row. Scale bar = 500 nm. (G) Apex of a late ribosome-rich sporoblast with a developing invasion apparatus (AD: anchoring disc; PTM: polar tube manubrium) and a polaroplast (P). Scale bar = 100 nm. (H) Uninucleate mature spore with a section of the polaroplast at the apex (LP: lamellar polaroplast; VP: vesicular polaroplast). PV: posterior vacuole; En: electron-lucent chitinous endospore; Ex: electron-dense exospore. Scale bar = 100 nm. (I) Spore cytoplasmic membrane (arrow) and spore wall composed of the endospore (En) and the exospore (Ex). A transversal section of the polar tube (arrowhead) is surrounded by the cytoplasm and the lamellar polaroplast (LP). Scale bar = 100 nm.

with *Msp1* and *Msp2*: the spore wall is twice as thick (140–150 nm for *O. duforti vs.* 55 and 80 nm for *Msp1* and *Msp2*, respectively) and the number of polar tube coils and rows is greater (2 rows, 8–11 coils for *O. duforti*, 1–2 rows, 6 coils for *Msp1* and 1 row, 4 coils for *Msp2*). *Msp1* and *Msp2* are also different from the other microsporidian species known to infect *Artemia*. *Nosema artemiae* is clearly different as it remains diplokaryotic during the whole cycle (Martinez *et al*. 1994). *Gurleya dispersa* and *Pleistophora myotropha* do not infect the gut but the haemocoel and muscle tissue, respectively (Codreanu, 1957). The spore sizes of both species are also larger (5·0–5·9 μm for *G. dispersa* and 5·5–6·9 μm for *P. myotropha*). Finally, *Vavraia anostraca* infects the haemocoel and musculature in addition to the gut (Martinez *et al*. 1992), and has different morphological features (merogonial division by plasmotomy, dimorphic oval spores with 2·8–3·5 μm-long microspores, anisofilar polar tube with 12–18 coils). Hence, this is the first report of *Msp1* and *Msp2* infection in *Artemia* species.

Characterization of Anostracospora rigaudi *n. g., n. sp. and* Enterocytospora artemiae *n. g., n. sp.*

Phylogenetic analyses based on the SSU rDNA revealed that *Msp1* and *Msp2* are related to three groups of microsporidia (Fig. 2). *Msp1* is included in the first group, along with various gut-infecting species and two species that do not infect gut epithelia (*Mrazekia macrocyclopis* and *Vittaforma corneae*; Silveira and Canning, 1995; Issi *et al*. 2010). Hence, we will only compare *Msp1* to other gut microsporidia from Group 1: *Endoreticulatus schubergi* (Cali and Garhy, 1991), *Cystosporogenes operophterae* (Canning *et al*. 1985; Canning and Curry, 2004), *Crispospora chironomi* (Tokarev *et al*. 2010) and *G. intestinalis* (Larsson *et al*. 1996). *Msp1* differs from these species as its parasitophorous vacuole develops only during sporogony. The number of sporoblasts in the parasitophorous vacuole is intermediate in *Msp1* (32–64) compared with *G. intestinalis* (16), *E. schubergi* (32) and *C. operophterae* (>128); no data are available for *C. chironomi*. *Msp1* has the smallest spores in the group (1·3 × 0·7 μm, compared with 2·5 × 1·5 μm for *E. schubergi*, 2·7 × 1·6 μm for *C. operophterae*, 2·4–2·7 × 1·1–1·7 μm for *G. intestinalis* and 2 × 1·5 μm/2·5 × 1·5 μm for the first and second type of spores of *C. chironomi*, respectively). The thickness of the spore wall of *Msp1* (55 nm) is comparable to that of *C. chironomi* (60 nm) and *E. schubergi* (50 nm), but thinner than the spore wall of *G. intestinalis* (80–85 nm) and C. *operophterae* (125 nm). *C. chironomi*, *G. intestinalis* and *Msp1* have few coils (4, 5 and 5–6, respectively), as compared with *E. schubergi* (7–9) and *C. operophterae* (10–12). The polar tube diameter is similar in *Msp1*, *C. chironomi* and *G. intestinalis* (60, 85 and 77–85 nm, respectively), but smaller than in *E. schubergi* (100 nm) and *C. operophterae* (120 nm). Interestingly, the parasitophorous vacuole of *Msp1* is persistent and remains intact when excreted with spores in the intestinal lumen. Such a persistent vacuole has also been described in *Cystosporogenes* (Kleespies *et al*. 2003), but is absent in the related *E. schubergi* where the fragile parasitophorous vacuole disappears in late sporogony (Cali and Garhy, 1991).

Msp2 is related to Group 1, 2 and 3 (Fig. 2). We compare *Msp2* to a subset of species from Groups 1, 2 and 3: *Msp1, G. intestinalis* (Larsson *et al*. 1996) (Group 1), *Desmozoon lepeophterii* (Freeman and Sommerville, 2009), *Enterocytozoon bieneusi* (Desportes *et al*. 1985), *E. hepatopenaei* (Tourtip *et al*. 2009), *Hepatospora eriocheir* (Stentiford *et al*. 2011) (Group 2), *Libermannia covasacrae* (Sokolova *et al*. 2009), *Orthosomella operophterae* (Canning, 1960) (outgroup in the phylogeny). In particular, we do not include *E. canceri* (Stentiford *et al*. 2007), *Nucleospora salmonis* (Chilmonczyk *et al*. 1991) and *Paranucleospora theridion* (Nylund *et al*. 2010) in this comparison as they infect cell nuclei. Merogony occurs within a parasitophorous vacuole in *Msp2, H. eriocheir, G. intestinalis* and *L. covasacrae*, whereas it occurs in direct contact with the host cell cytoplasm in *Msp1, O. operophterae* and in other species from Group 2. Hence, this character appears to evolve very quickly in this lineage. Meronts are unikaryotic in *Msp2* as in all other species considered except *D. lepeophterii* and *L. covasacrae*. Merogonial division is by binary fission in *Msp1, Msp2* and *L. covasacrae*, contrary to all other species where it occurs by plasmotomy, by rosette-like division (*H. eriocheir*) or by binary fission followed by plasmotomy (*D. lepeophterii*). The sporogonial division is by plasmotomy in *Msp1, Msp2*, and all other species considered, except in *E. hepatopenaei*, and *L. covasacrae* where it occurs by binary fission. The development of the invasion apparatus occurs in isolated sporoblasts in *Msp1, Msp2, G. intestinalis, D. lepeophterii, L. covasacrae* and *O. operophterae*, while it starts in the sporogonial plasmodium in *E. bieneusi, E. hepatopenaei* and *E. canceri*. The number of sporoblasts within the parasitophorous vacuole is greater in *Msp2* (64–128) compared with *Msp1* (32–64), *O. operophterae* (12), and *G. intestinalis* (16) (no data available for *E. hepatopenaei, H. eriocheir, D. lepeophterii, E. bieneusi* and *L. covasacrae*). *Msp2* spores are subspherical (1·2 × 0·9 μm) and have lower eccentricity than the more oval *Msp1* spores (1·3 × 0·7 μm). *Msp2* and *E. hepatopenaei* (1·1 × 0·7 μm) have the smallest spore size compared with all other species considered (1·5 × 0·8 μm for *E. bineusi*, 1·7 × 1·0 μm for *H. eriocheir*, 2·2–3·4 × 1·1–1·7 μm for *L. covasacrae*, 2·3 × 1·8 μm for *D. lepeophterii*, 2·4–2·7 × 1·1–1·7 μm for *G. intestinalis*, 3·5 × 1·2 μm for *O. operophterae*).

The thickness of the spore wall is similar in *Msp1, O. operophterae, E. hepatopenaei* and *H. eriocheir* (50–55 nm) and larger in all other species (*D. lepeophterii*: 75 nm, *Msp2*: 80 nm, *G. intestinalis*: 80–85 nm, *L. covasacrae*: 120 nm), except *E. bieneusi* (30–35 nm). The polar tubes of *Msp2, H. eriocheir* and *L. covasacrae* are the thickest (diameters 100, 120 and 120 nm respectively), compared with *Msp1* (70 nm), *D. lepeophterii* (65–85 nm), *E. bieneusi* (75 nm), *O. operophterae* (75 nm), *G. intestinalis* (77–85 nm) and *E. hepatopenaei* (90 nm). The number of polar tube coils is small in *Msp2* (4), *L. covasacrae* (3–5) and *E. bieneusi* (4–7), as compared with *Msp1* and *E. hepatopenaei* (5–6), *D. lepeophterii* and *G. intestinalis* (5–8), *O. operophterae* (6–7) and *H. eriocheir* (7–8).

Based on molecular and ultrastructural evidence, *Msp1* and *Msp2* have not been previously described and constitute new species. We propose to name them *Anostracospora rigaudi* and *Enterocytospora artemiae* respectively. Both species are likely to be exclusively horizontally transmitted, given the rate of horizontal transmission observed in the laboratory (> 50%) and the lack of infection detected in nauplii produced by infected mothers (although we cannot completely rule out the possibility of low-level vertical transmission in *E. artemiae*). As spores are released into the intestinal lumen while the host is alive, transmission probably occurs among living hosts. In this case, new hosts are infected by filter-feeding spores in the water column, as in related microsporidia (Ebert, 1994; Ebert *et al*. 2000). This study illustrates the usefulness of molecular markers to characterize and discriminate among microsporidia infecting gut tissues.

Taxonomic summary for Anostracospora rigaudi *n. g., n. sp.* (Msp1)

Phylum: Microsporidia Balbiani, 1882

Family: incertae sedis

Genus: Anostracospora n. g.

Closely related to the genera *Endoreticulatus* and *Cystosporogenes*, based on SSU rDNA phylogeny (Fig. 2). All life cycle stages with isolated nuclei. Merogony in direct contact with host cell cytoplasm. Sporogony by plasmotomy within a parasitophorous vacuole. Meiosis not observed. Mature spores ovoid. Polar tube isofilar. No production of xenomas.

Type species: *Anostracospora rigaudi* n. sp.

Type hosts: *Artemia franciscana* Kellogg, 1906, *A. parthenogenetica* Bowen and Sterling, 1978.

Prevalence of infection: 39·5% (58/147) in *A. franciscana*, 75·2% in *A. parthenogenetica* (100/133). Prevalence based on samples collected in 2008 in Aigues-Mortes, France.

Phenotypic effects: Strong negative effect on the probability of reproduction in female hosts (Rode *et al*. in press). Effect on host survival not studied. Strong positive effect on host swarming and surfacing behaviour (Rode *et al*. 2013).

Locality: Southern France, Ukraine (Rode *et al*. in press)

Genbank accession: JX915758, JX915759 (Aigues-Mortes, Fance).

Transmission: Horizontal transmission, most likely with the faeces of infected individuals.

Site of infection: Intestinal epithelium, no production of syncytia or xenomas. Infection is characteristically found in the zone between the brush border and the nucleus. Infected cells are not hypertrophied.

Merogony: Uninucleate meronts develop in direct contact with host cytoplasm (unknown mode of division).

Sporogony: Uninucleate sporonts divide by plasmotomy within a parasitophorous vacuole. Asynchronous development with meronts and sporonts found in the same vacuole. The parasitophorous vacuole including mature spores is released intact into the gut lumen.

Spore: Mature spores uninucleate, ovoid and small (1·3 × 0·7 μm). The spore wall is 55-nm thick. The polar tube is isofilar with 5–6 coils (diameter: 60 nm) arranged in one or two rows of coils.

Parasitophorous vacuole: Initiated at the beginning of sporogony.

Types: Syntypes in resin block No. PC0709125, on slide No. PC0709126 and copper grid No. PC0709127.

Deposition of types: Resin block No. PC0709125 (infected *A. parthenogenetica* female specimen), slide No. PC0709126 (intestinal semi-thin sections of an infected *A. parthenogenetica* female) and copper grid No. PC0709127 (intestinal ultra-thin sections of an infected *A. parthenogenetica* female showing developing and mature spores) were deposited in the collection of the Muséum National d'Histoire Naturelle (MNHN), 75231, Paris, France.

Etymology: Genus named after the order Anostraca Sars, 1867. Species named after Thierry Rigaud who kindly conducted the first PCR tests to check microsporidian infection in *Artemia* spp.

Taxonomic summary for Enterocytospora artemiae *n. g., n. sp.* (Msp2)

Phylum: Microsporidia Balbiani, 1882

Family: incertae sedis

Genus: Enterocytospora n. g.

Polytomous position with two different groups including the genera *Endoreticulatus* and *Enterocytozoon* based on SSU rDNA phylogeny (Fig. S1 – in Online version only). All life cycle stages with isolated nuclei. Merogonial reproduction by binary division within a parasitophorous vacuole. Sporogony by plasmotomy within a parasitophorous vacuole. Meiosis not observed. Mature spores

subspherical. Polar tube isofilar. No production of xenomas.

Type species: *Enterocytospora artemiae* n. sp.

Type hosts: *Artemia franciscana* Kellogg, 1906, *A. franciscana monica* Verrill, 1869, *A. parthenogenetica* Bowen and Sterling, 1978.

Prevalence of infection: 52·4% (77/147) in *A. franciscana*, 21·8% in *A. parthenogenetica* (29/133). Prevalence based on samples collected in 2008 in Aigues-Mortes, France.

Phenotypic effects: No effect on the probability of reproduction in female hosts (Rode *et al*. submitted). Effect on host survival not studied. Strong positive effect on host swarming and surfacing behaviour (Rode *et al*. 2013).

Locality: Southern France; Mono Lake, CA, USA; Great Salt Lake, UT, USA; Eilat and Ein Evrona salterns, Eilat, Israel (Rode *et al*. submitted).

Genbank accession: JX915760 (Aigues-Mortes, France), JX839889 and JX915761 (Great Salt Lake, UT, USA), JX915754 and JX915755 (Mono Lake, CA, USA), JX915756 and JX915757 (Ein Evrona, Eilat, Israel).

Transmission: Horizontal transmission, most likely with the faeces of infected individuals.

Site of infection: Intestinal epithelium, no production of syncytia or xenomas. Infection is characteristically found in the zone between the brush border and the nucleus. Infected cells are not hypertrophied.

Merogony: Uninucleate meronts divide by binary fission within a parasitophorous vacuole.

Sporogony: Uninucleate sporonts divide by plasmotomy within a parasitophorous vacuole. Asynchronous development with meronts, sporonts and sporoblasts found together within the parasitophorous vacuole. Development of sporoblasts and mature spores together within the parasitophorous vacuole. The parasitophorous vacuole, including mature spores, is released intact into the gut lumen.

Spore: Mature spores uninucleate, subspherical and small (1·2 × 0·9 μm). Spore wall is 80-nm thick. The polar tube is isofilar with 4 coils (diameter: 100 nm) arranged in one row of coils.

Parasitophorous vacuole: Initiated at the beginning of merogony.

Types: Syntypes in resin block No. PC0709128, on slide No. PC0709129 and copper grid No. PC0709130.

Deposition of types: Resin block No. PC0709128 (infected *A. franciscana* female specimen), slide No. PC0709129 (intestinal semi-thin sections of an infected *A. franciscana* female) and copper grid No. PC0709130 (intestinal ultra-thin sections of an infected *A. franciscana* female showing developing and mature spores) were deposited in the collection of the MNHN, 75231, Paris, France.

Etymology: Genus name describes the site of infection. Specific epithet describes host genus.

Detection of cryptic infection

Obtaining accurate and reliable estimates of parasite prevalence in the field is a prerequisite to the study of their ecology and their impact on host populations. However, infection by gut microsporidia is often cryptic as they often leave no macroscopic traces in their host (Ebert, 2005) and because they can be difficult to distinguish from the intestinal flora (especially when their size is similar to bacteria, as is the case for the two species described here). Even for species with larger spores, such as *U. exiguum*, their prevalence in natural populations is difficult to estimate (Codreanu, 1957). We developed species-specific molecular markers and investigated the phenotypes of hosts infected by *A. rigaudi* or *E. artemiae*. Surprisingly, we found no significant association between infection by either parasite and the presence of white-spots on the cuticle or posterior part of the digestive tract. Thus, this cue is not associated with *A. rigaudi* or *E. artemiae* infection. These white-spots could represent infections by other microsporidian species or viruses known to produce white spots in *Artemia* and other crustacean hosts (Li *et al*. 2003; Escobedo-Bonilla *et al*. 2008). Macroscopic symptoms of infection such as 'white-spots' could in principle be an attractive method to measure microsporidian prevalence in *Artemia* populations, provided that a non-ambiguous association is made with infection of a given stage of the relevant parasite(s). As far as we know, this has not been clearly demonstrated, even if *N. artemiae* and *V. anostraca* are probably responsible for these 'white-spots' (Codreanu, 1957; Martinez *et al*. 1992, 1994). Hence, PCR assays with specific markers such as those developed in this and other studies (e.g. Hogg *et al*. 2002; Weigl *et al*. 2012) remain the most accurate method to reliably detect microsporidian infections and to accurately estimate their prevalence in the field. In addition, these molecular techniques allow morphologically similar species to be distinguished within 3–6 days of hosts being infected. A similar time-to-detection period has been found in a *Nosema* species infecting silkworms (Hatakeyama and Hayasaka, 2002). This period likely corresponds to the time necessary for spore germination and meront multiplication before microsporidian DNA can be detected by PCR.

In conclusion, we report the existence of and characterize two new microsporidian species. Despite their prevalence, these cryptic species have remained unnoticed for several reasons: (1) they do not cause macroscopic symptoms, (2) they are localized in the intestinal tract, and are mixed with a diversity of other microorganisms when directly observed on *Artemia* squashes, (3) they are small enough to be confounded with bacteria in the same size range, (4) they grow in the intestinal epithelium which is renewed with each host moult, preventing their

proliferation to some extent. We developed molecular markers to detect their presence and discriminate between these two similar species. These methods offer a useful complement to microscopic techniques to study the ecology and evolution of these important but cryptic intracellular parasites.

ACKNOWLEDGEMENTS

The authors are grateful to C. Cazevieille and C. Sanchez for their technical assistance. We thank T. Rigaud and M.-P. Dubois for their advice and help regarding the molecular and microscopic investigations of microsporidiosis. We also thank three anonymous reviewers for their useful comments.

FINANCIAL SUPPORT

Financial support was provided by the QuantEvol ERC grant (T. L.) and a French Ministry of Research fellowship (N. O. R.).

REFERENCES

Baker, M. D., Vossbrinck, C. R., Maddox, J. V. and Undeen, A. H. (1994). Phylogenetic relationships among *Vairimorpha* and *Nosema* species (Microspora) based on ribosomal RNA sequence data. *Journal of Invertebrate Pathology* **30**, 509–518.

Becnel, J. J. (1992). Horizontal transmission and subsequent development of *Amblyospora californica* (Microsporida: Amblyosporidae) in the intermediate and definitive hosts. *Diseases of Aquatic Organisms* **13**, 17–28.

Cali, A. and Garhy, M. E. L. (1991). Ultrastructural study of the development of *Pleistophora schubergi* Zwölfer, 1927 (Protozoa, Microsporida) in larvae of the spruce budworm, *Choristoneura fumiferana* and its subsequent taxonomic change to the genus *Endoreticulatus*. *Journal of Eukaryotic Microbiology* **38**, 271–278.

Canning, E. U. (1960). Two new microsporidian parasites of the winter moth, *Operophtera brumata* (L.). *Journal of Parasitology* **46**, 755–763.

Canning, E. U. and Vávra, J. (2000). Phylum Microsporidia Balbiani, 1882. In *The Illustrated Guide to the Protozoa* (ed. Lee, J. J., Leedale, G. F. and Bradbury, P.), pp. 39–126. Allen Press, Lawrence, KS.

Canning, E. U. and Curry, A. (2004). Further observations on the ultrastructure of *Cystosporogenes operophterae* (Canning, 1960) (phylum Microsporidia) parasitic in *Operophtera brumata* L. (Lepidoptera, Geometridae). *Journal of Invertebrate Pathology* **87**, 1–7.

Canning, E. U., Barker, R. J., Nicholas, J. P. and Page, A. M. (1985). The ultrastructure of three microsporidia from winter moth, *Operophtera brumata* (L.), and the establishment of a new genus *Cystosporogenes* n. g. for *Pleistophora operophterae* (Canning, 1960). *Systematic Parasitology* **7**, 213–225.

Castresana, J. (2000). Selection of conserved blocks from multiple alignments for their use in phylogenetic analysis. *Molecular Biology and Evolution* **17**, 540–552.

Chilmonczyk, S., Cox, W. T. and Hedrick, R. P. (1991). *Enterocytozoon salmonis* n. sp.: an intranuclear microsporidium from salmonid fish. *Journal of Eukaryotic Microbiology* **38**, 264–269.

Codreanu, R. (1957). Sur quatre espèces nouvelles de microsporidies parasites de l'*Artemia salina* (L.) de Roumanie. *Annales Des Sciences Naturelles Zoologiques* **19**, 561–572.

Codreanu, R. and Codreanu-Balcescu, D. (1980). Parasitoses massives des populations du crustacé *Artemia salina* et du chironomide *Halliella noctivaga* dominantes dans la faune du lac sursalé Tékirghiol. *Muz. St. Constata, Pontus Euxinus Studiisi Cercetari* **1**, 305–314.

Darriba, D., Taboada, G. L., Doallo, R. and Posada, D. (2012). jModelTest 2: more models, new heuristics and parallel computing. *Nature Methods* **9**, 772.

Desportes, I., Charpentier, Y. L., Galian, A., Bernard, F., Cochand-Priollet, B., Lavergne, A., Ravisse, P. and Modigliani, R. (1985). Occurrence of a new microsporidan: *Enterocytozoon bieneusi* n. g., n. sp., in the enterocytes of a human patient with AIDS. *Journal of Eukaryotic Microbiology* **32**, 250–254.

Dunn, A. and Hatcher, M. (1997). Prevalence, transmission and intensity of infection by a microsporidian sex ratio distorter in natural *Gammarus duebeni* populations. *Parasitology* **114**, 231–236.

Ebert, D. (1994). Genetic differences in the interactions of a microsporidian parasite and four clones of its cyclically parthenogenetic host. *Parasitology* **108**, 11–16.

Ebert, D. (2005). *Ecology, Epidemiology, and Evolution of Parasitism in Daphnia* [Internet], National Center for Biotechnology Information, Bethesda, MD, USA. http://www.ncbi.nlm.nih.gov/books/NBK2036/.

Ebert, D., Lipsitch, M. and Mangin, K. L. (2000). The effect of parasites on host population density and extinction: experimental epidemiology with *Daphnia* and six microparasites. *American Naturalist* **156**, 459–477.

Escobedo-Bonilla, C., Alday-Sanz, V., Wille, M., Sorgeloos, P., Pensaert, M. and Nauwynck, H. (2008). A review on the morphology, molecular characterization, morphogenesis and pathogenesis of white spot syndrome virus. *Journal of Fish Diseases* **31**, 1–18.

Folmer, O., Black, M., Hoeh, W., Lutz, R. and Vrijenhoek, R. (1994). DNA primers for amplification of mitochondrial cytochrome c oxidase subunit I from diverse metazoan invertebrates. *Molecular Marine Biology and Biotechnology* **3**, 294–299.

Freeman, M. A. and Sommerville, C. (2009). *Desmozoon lepeophtherii* n. gen., n. sp. (Microsporidia: Enterocytozoonidae) infecting the salmon louse *Lepeophtheirus salmonis* (Copepoda: Caligidae). *Parasites and Vectors* **2**, 1–15.

Gatehouse, H. S. and Malone, L. A. (1998). The ribosomal RNA gene region of *Nosema apis* (Microspora): DNA sequence for small and large subunit rRNA genes and evidence of a large tandem repeat unit size. *Journal of Invertebrate Pathology* **71**, 97–105. doi: 10.1006/jipa.1997.4737.

Guindon, S. and Gascuel, O. (2003). A simple, fast, and accurate algorithm to estimate large phylogenies by maximum likelihood. *Systematic Biology* **52**, 696–704. doi: 10.1080/10635150390235520.

Guindon, S., Dufayard, J. F., Lefort, V., Anisimova, M., Hordijk, W. and Gascuel, O. (2010). New algorithms and methods to estimate maximum-likelihood phylogenies: assessing the performance of PhyML 3.0. *Systematic Biology* **59**, 307–321.

Hatakeyama, Y. and Hayasaka, S. (2002). Specific amplification of microsporidian DNA fragments using multiprimer PCR. *Japan Agricultural Research Quarterly* **36**, 97–102.

Hogg, J., Ironside, J., Sharpe, R., Hatcher, M., Smith, J. and Dunn, A. (2002). Infection of *Gammarus duebeni* populations by two vertically transmitted microsporidia; parasite detection and discrimination by PCR–RFLP. *Parasitology* **125**, 59–63.

Issi, I. V., Tokarev, Y. S., Voronin, V. N., Seliverstova, E. V., Pavlova, O. A. and Dolgikh, V. V. (2010). Ultrastructure and molecular phylogeny of *Mrazekia macrocyclopis* sp. n. (Microsporidia, Mrazekiidae), a microsporidian parasite of *Macrocyclops albidus* (Jur.) (Crustacea, Copepoda). *Acta Protozoologica* **49**, 75–84.

Kleespies, R. G., Vossbrinck, C. R., Lange, M. and Jehle, J. A. (2003). Morphological and molecular investigations of a microsporidium infecting the European grape vine moth, *Lobesia botrana* Den. et Schiff., and its taxonomic determination as *Cystosporogenes legeri* nov. comb. *Journal of Invertebrate Pathology* **83**, 240–248.

Larsson, J. I. R., Ebert, D., Vávra, J. and Voronin, V. (1996). Redescription of *Pleistophora intestinalis* Chatton, 1907, a microsporidian parasite of *Daphnia magna* and *Daphnia pulex*, with establishment of the new genus *Glugoides* (Microspora, Glugeidae). *European Journal of Protistology* **32**, 251–259.

Larsson, J. I. R., Ebert, D. and Vávra, J. (1997). Ultrastructural study and description of *Ordospora colligata* gen. et sp. nov. (Microspora, Ordosporidae fam. nov.), a new microsporidian parasite of *Daphnia magna* (Crustacea, Cladocera). *European Journal of Protistology* **33**, 432–443.

Li, Q., Zhang, J., Chen, Y. and Yang, F. (2003). White spot syndrome virus (WSSV) infectivity for *Artemia* at different developmental stages. *Diseases of Aquatic Organisms* **57**, 261–264.

Martinez, M. A., Larsson, J. I. R. and Morales, J. (1989). Morphological, pathological and ecological data of a microsporidium of the genus *Nosema* on *Artemia*. *Aquaculture Europe'89. Short Communications. Special Publication of E. A. C.* **10**, 161–163.

Martinez, M. A., Vivarès, C. P., Rocha, R. D., Fonseca, A. C., Andral, B. and Bouix, G. (1992). Microsporidiosis on *Artemia* (Crustacea, Anostraca): light and electron microscopy of *Vavraia anostraca* sp. nov. (Microsporidia, Pleistophoridae) in the Brazilian solar salterns. *Aquaculture* **107**, 229–237.

Martinez, M. A., Vivarès, C. P. and Bouix, G. (1993). Ultrastructural study of *Endoreticulatus durforti* n. sp., a new microsporidian parasite of the intestinal epithelium of *Artemia* (Crustacea, Anostraca). *Journal of Eukaryotic Microbiology* **40**, 677–687.

Martinez, M. A., Larsson, J. I. R., Amat, F. and Vivarès, C. P. (1994). Cytological study of *Nosema artemiae* (Codreanu, 1957) Sprague, 1977 (Microsporidia, Nosematidae). *Archiv für Protistenkunde* **144**, 83–89.

Molina, J. M., Sarfati, C., Beauvais, B., Lémann, M., Lesourd, A., Ferchal, F., Casin, I., Lagrange, P., Modigliani, R. and Derouin, F. (1993). Intestinal microsporidiosis in human immunodeficiency virus-infected patients with chronic unexplained diarrhea: prevalence and clinical and biologic features. *Journal of Infectious Diseases* **167**, 217–221.

Muñoz, J., Green, A., Figuerola, J., Amat, F. and Rico, C. (2008). Characterization of polymorphic microsatellite markers in the brine shrimp *Artemia* (Branchiopoda, Anostraca). *Molecular Ecology Resources* **9**, 547–550.

Nylund, S., Nylund, A., Watanabe, K., Arnesen, C. E. and Karlsbakk, E. (2010). *Paranucleospora theridion* n. gen., n. sp. (Microsporidia, Enterocytozoonidae) with a life cycle in the salmon louse (*Lepeophtheirus salmonis*, Copepoda) and Atlantic salmon (*Salmo salar*). *Journal of Eukaryotic Microbiology* **57**, 95–114.

Otti, O. and Schmid-Hempel, P. (2008). A field experiment on the effect of *Nosema bombi* in colonies of the bumblebee *Bombus terrestris*. *Ecological Entomology* **33**, 577–582.

Ovcharenko, M. and Wita, I. (2005). The ultrastructural study of *Nosema artemiae* (Codreanu, 1957) (Microsporidia: Nosematidae). *Acta Protozoologica* **44**, 33–41.

Rode, N. O., Lievens, E. J. P., Flaven, E., Segard, A., Jabbour-Zahab, R., Sanchez, M. I. and Lenormand, T. (2013). Why join groups? Lessons from parasite-manipulated *Artemia*. *Ecology Letters* **16**, 493–501.

Rode, N. O., Lievens, E. J. P., Flaven, E., Segard, A., Jabbour-Zahab, R. and Lenormand, T. Cryptic microsporidian parasites differentially affect invasive and native *Artemia* spp. *International Journal for Parasitology*, in press.

Ryan, J. A. and Kohler, S. L. (2010). Virulence is context-dependent in a vertically transmitted aquatic host–microparasite system. *International Journal for Parasitology* **40**, 1665–1673.

Silveira, H. and Canning, E. U. (1995). *Vittaforma corneae* n. comb. for the human microsporidium *Nosema corneum* Shadduck, Meccoli, Davis & Font, 1990, based on its ultrastructure in the liver of experimentally infected athymic mice. *Journal of Eukaryotic Microbiology* **42**, 158–165.

Sokolova, Y. Y., Lange, C. E., Mariottini, Y. and Fuxa, J. R. (2009). Morphology and taxonomy of the microsporidium *Liebermannia covasacrae* n. sp. from the grasshopper *Covasacris pallidinota* (Orthoptera, Acrididae). *Journal of Invertebrate Pathology* **101**, 34–42.

Stentiford, G. D., Bateman, K. S., Longshaw, M. and Feist, S. W. (2007). *Enterospora canceri* n. gen., n. sp., intranuclear within the hepatopancreatocytes of the European edible crab *Cancer pagurus*. *Diseases of Aquatic Organisms* **75**, 61–72. doi: 10.3354/dao075061.

Stentiford, G. D., Bateman, K. S., Small, H. J., Moss, J., Shields, J. D., Reece, K. S. and Tuck, I. (2010). *Myospora metanephrops* (n. g., n. sp.) from marine lobsters and a proposal for erection of a new order and family (Crustaceacida; Myosporidae) in the Class Marinosporidia (Phylum Microsporidia). *International Journal for Parasitology* **40**, 1433–1446. doi: 10.1016/j.ijpara.2010.04.017.

Stentiford, G. D., Bateman, K. S., Dubuffet, A., Chambers, E. and Stone, D. M. (2011). *Hepatospora eriocheir* (Wang and Chen, 2007) gen. et comb. nov. infecting invasive Chinese mitten crabs (*Eriocheir sinensis*) in Europe. *Journal of Invertebrate Pathology* **108**, 156–166. doi: 10.1016/j.jip.2011.07.008.

Stirnadel, H. A. and Ebert, D. (1997). Prevalence, host specificity and impact on host fecundity of microparasites and epibionts in three sympatric *Daphnia* species. *Journal of Animal Ecology* **66**, 212–222.

Tamura, K., Peterson, D., Peterson, N., Stecher, G., Nei, M. and Kumar, S. (2011). MEGA5: molecular evolutionary genetics analysis using maximum likelihood, evolutionary distance, and maximum parsimony methods. *Molecular Biology and Evolution* **28**, 2731–2739. doi: 10.1093/molbev/msr121.

Texier, C., Vidau, C., Viguès, B., El Alaoui, H. and Delbac, F. (2010). Microsporidia: a model for minimal parasite–host interactions. *Current Opinion in Microbiology* **13**, 443–449. doi: 10.1016/j.mib.2010.05.005.

Thomarat, F., Vivares, C. P. and Gouy, M. (2004). Phylogenetic analysis of the complete genome sequence of *Encephalitozoon cuniculi* supports the fungal origin of microsporidia and reveals a high frequency of fast-evolving genes. *Journal of Molecular Evolution* **59**, 780–791. doi: 10.1007/s00239-004-2673-0.

Tokarev, Y. S., Voronin, V. N., Seliverstova, E. V., Pavlova, O. A. and Issi, I. V. (2010). Life cycle, ultrastructure, and molecular phylogeny of *Crispospora chironomi* g. n. sp. n. (Microsporidia: Terresporidia), a parasite of *Chironomus plumosus* L. (Diptera: Chironomidae). *Parasitology Research* **107**, 1381–1389.

Tourtip, S., Wongtripop, S., Stentiford, G. D., Bateman, K. S., Sriurairatana, S., Chavadej, J., Sritunyalucksana, K. and Withyachumnarnkul, B. (2009). *Enterocytozoon hepatopenaei* sp. nov. (Microsporida: Enterocytozoonidae), a parasite of the black tiger shrimp *Penaeus monodon* (Decapoda: Penaeidae): Fine structure and phylogenetic relationships. *Journal of Invertebrate Pathology* **102**, 21–29. doi: 10.1016/j.jip.2009.06.004.

Vossbrinck, C. R. and Debrunner-Vossbrinck, B. A. (2005). Molecular phylogeny of the Microsporidia: ecological, ultrastructural and taxonomic considerations. *Folia Parasitologica* **52**, 131–142.

Vossbrinck, C. R., Andreadis, T. G. and Weiss, L. M. (2004). Phylogenetics: taxonomy and the microsporidia as derived fungi. In *Opportunistic Infections: Toxoplasma, Sarcocystis, and Microsporidia*, Vol. 9 (ed. Lindsay, D. S. and Weiss, L. M.), pp. 189–213. Springer, New York, USA.

Vossbrinck, C. R., Baker, M. D., Didier, E. S., Debrunner-Vossbrinck, B. A. and Shadduck, J. A. (1993). Ribosomal DNA sequences of *Encephalitozoon hellem* and *Encephalitozoon cuniculi*: species identification and phylogenetic construction. *Journal of Eukaryotic Microbiology* **40**, 354–362.

Wang, C. Y., Solter, L. F., T'sui, W. H. and Wang, C. H. (2005). An *Endoreticulatus* species from *Ocinara lida* (Lepidoptera: Bombycidae) in Taiwan. *Journal of Invertebrate Pathology* **89**, 123–135.

Weigl, S., Körner, H., Petrusek, A., Seda, J., Wolinska, J., Becnel, J., Andreadis, T., Wittner, M., Weiss, L. and Ben-Ami, F. (2012). Natural distribution and co-infection patterns of microsporidia parasites in the *Daphnia longispina* complex. *Parasitology–Cambridge* **139**, 870–880.

Weiss, L. M. (2005). The first united workshop on microsporidia from invertebrate and vertebrate hosts. *Folia Parasitologica* **52**, 1–7.

Weiss, L. M., Zhu, X., Cali, A., Tanowitz, H. B. and Wittner, M. (1994). Utility of microsporidian rRNA in diagnosis and phylogeny – a review. *Folia Parasitologica* **41**, 81–90.

Supplementary data

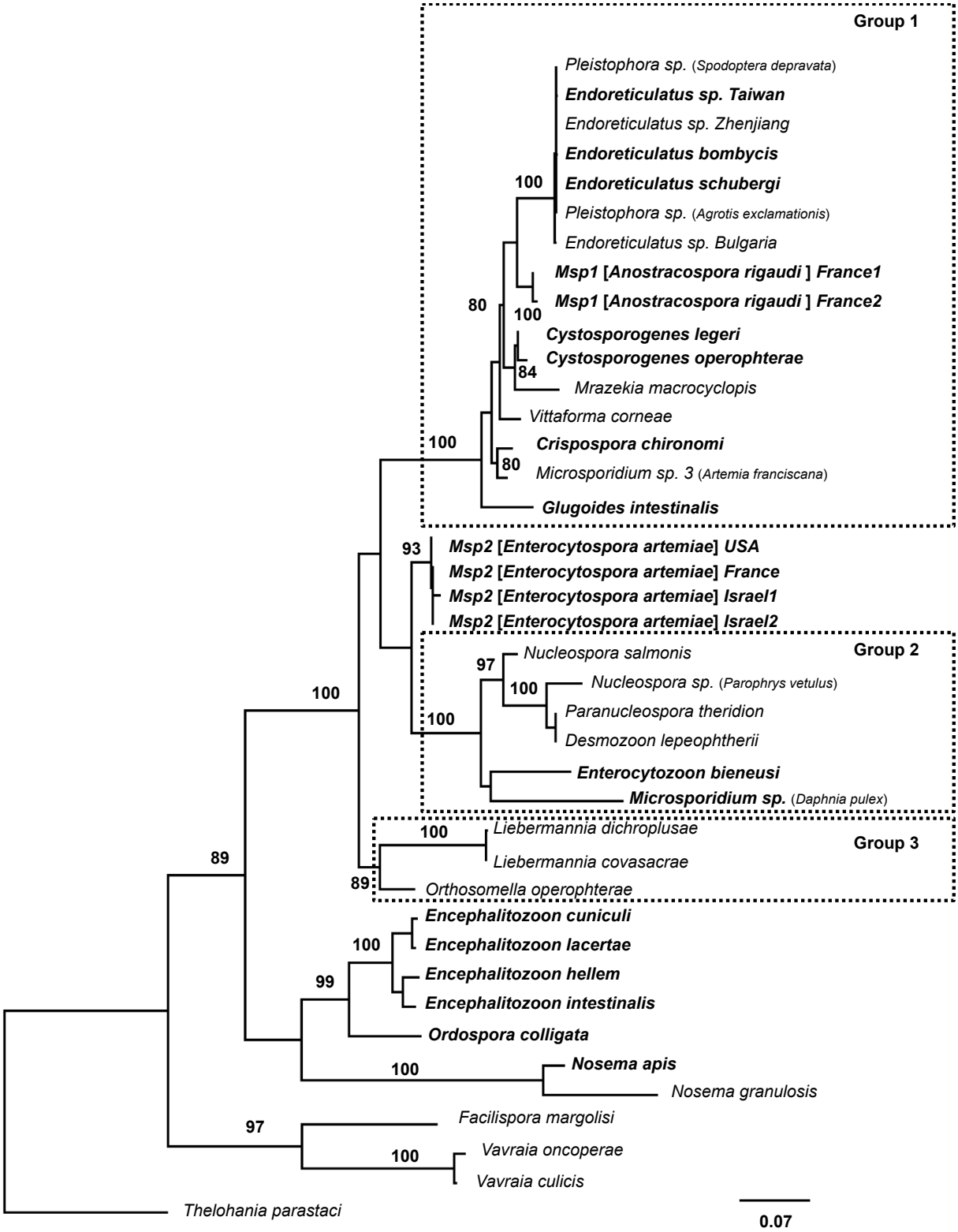

Fig. S1. Maximum likelihood tree of the SSU rDNA of *Msp1* (*Anostracospora rigaudi*) and *Msp2* (*Enterocytospora artemiae*) along with related microsporidian species infecting crustacean and non-crustacean hosts (excluding the following short sequences: *Hepatospora* spp., *Enterospora canceri, Enterocytozoon hepatopenaei* and *Myospora metanephrops*, final length ~720bp). Names of species infecting the digestive tract epithelium appear in bold. The host species of undescribed microsporidia appear between parentheses. Numbers above branches indicate bootstrap supports from 100 resamplings (only values above 80 are reported). Bootstrap support for the node showing *Msp2* as a sister species to Group 2 was very low (45%).

Table S1. List of microsporidian sequences used for the SSU rDNA phylogenetic analyses.

Organism	GenBank Acc. Number
Crispospora chironomi	GU130407
Cystosporogenes legeri	AY233131
Cystosporogenes operophterae	AJ302320
Desmozoon lepeophtherii	HM800847
Encephalitozoon cuniculi	L39107
Encephalitozoon hellem	L39108
Encephalitozoon intestinalis	L39113
Encephalitozoon lacertae	AF067144
Endoreticulatus schubergi	L39109
Endoreticulatus bombycis	AY009115
Endoreticulatus sp. Bulgaria	AY502945
Endoreticulatus sp. Taiwan	AY502944
Endoreticulatus sp. Zhenjiang	FJ772431
Enterocytozoon bieneusi	L07123
Enterocytozoon hepatopenaei	FJ496356
Enterospora canceri	HE584634
Facilispora margolisi	HM800849
Glugoides intestinalis	AF394525
Hepatospora eriocheir	HE584635
Hepatospora sp. (Cancer Pagarus)	HE584633
Liebermannia covasacrae	EU709818
Liebermannia dichroplusae	EF016249
Microsporidium sp. (Daphnia pulex)	AF394528
Microsporidium sp. 1 France1	JX915758
Microsporidium sp. 1 France2	JX915759
Microsporidium sp. 2 France	JX915760
Microsporidium sp. 2 Israel1	JX915756
Microsporidium sp. 2 Israel2	JX915757
Microsporidium sp. 2 USA	JX839889
Microsporidium sp. 3 (Artemia franciscana)	JX839890
Mrazekia macrocyclopis	FJ914315
Myospora metanephrops	HM140497
Nosema apis	X73894
Nosema granulosis	FN434088
Nucleospora sp. (Parophrys vetulus)	AF186007
Nucleospora salmonis	U78176
Ordospora colligata	AF394529
Orthosomella operophterae	AJ302317
Paranucleospora theridion	FJ594990
Pleistophora sp. (Agrotis exclamationis)	U10342
Pleistophora sp. (Spodoptera depravata)	D85500
Thelohania parastaci	AF294781
Vavraia culicis	AJ252961
Vavraia oncoperae	X74112
Vittaforma corneae	L39112

Table S2. Mean genetic distances between *Msp1, Endoreticulatus* spp.*, Cystosporogenes* spp.*,* the remaining species from Group 1 ("Others in Group 1") and *Msp2*.

	Msp1	***Endoreticulatus***	***Cystosporogenes***	**Others in Group1**
Msp1				
Endoreticulatus	0.035			
Cystosporogenes	0.066	0.048		
Others in Group1	0.060	0.047	0.060	
Msp2	0.134	0.103	0.143	0.125

Table S3. Mean genetic distances between *Msp2* and all major clades from the phylogeny in Fig. S1.

	Group1	***Msp2***	***Group2***	***Group3***	***Encephalitozoon/ Ordospora***	***Nosema***
Group1						
Msp2	0.117					
Group2	0.225	0.163				
Group3	0.185	0.145	0.219			
Encephalitozoon/ Ordospora	0.248	0.190	0.284	0.237		
Nosema	0.328	0.303	0.399	0.378	0.329	
Vavraia	0.418	0.392	0.439	0.402	0.414	0.505

Table S4. Comparison of the different gut microsporidia related to *Msp1* (*Anacostracospora rigaudi*) and *Msp2* (*Enterocytospora artemiae*)

Microsporidian species	Host	Distribution	Site of infection	Parasitophorous vacuole	Meront nuclei
Anacostracospora rigaudi	Anostraca: Artemia	Southern France, Ukraine	Intestinal epithelium	Appears during sporogony	Monokaryotic
Enterocytospora artemiae	Anostraca: Artemia	Southern France, Israel, USA	Intestinal epithelium	Appears during merogony	Monokaryotic
Ordospora duforti	Anostraca: Artemia	Spain	Intestinal epithelium	Appears during merogony	Monokaryotic
Vavria anostraca	Anostraca: Artemia	Brazil	Intestinal epithelium, muscle	Appears during sporogony	Monokaryotic
Glugoides intestinalis	Cladocera: Daphnia	Europe	Intestinal epithelium	Appears during merogony	Monokaryotic
Cystosporogenes operophterae	Lepidoptera: Operophtera	UK	Salivary glands, intestinal epithelium	Appears during merogony	Monokaryotic
Endoreticulatus schubergi	Lepidoptera: Choristoneura	USA	Intestinal epithelium	Appears during merogony	Monokaryotic
Crispospora chironomi	Diptera: Chironoma	Russia	Intestinal epithelium	Appears during merogony	Diplokaryotic
Orthosomella operophterae	Lepidoptera: Operophtera	UK, USA	Silk gland, intestinal epithelium and other tissues	None	Monokaryotic
Desmozoon lepeophtherii	Copepod: Lepeophtheirus	UK	Desmocyte	None	Diplokaryotic
Enterocytozoon bieneusi	Primates: Homo	worldwide	Intestinal epithelium	None	Unikaryotic
Enterocytozoon hepatopenaei	Decapoda: Penaeus	Thailand	Hepatopancreas epithelium	None	unknown
Enterospora canceri	Decapoda: Cancer	UK	Hepatopancreatocytes nucleoplasm	Appears during merogony	unknown
Hepatospora eriocheir	Decapoda: Eriocheir	UK, China	Hepatopancreas epithelium	Appears during merogony	Monokaryotic
Liebermannia covasacrae	Orthoptera: Covasacris	Argentina	Salivary gland	Appears during merogony	Diplokaryotic

Table S4. (continued)

Microsporidian species	Merogonial division	Sporont nuclei	Sporogonial division	Number of sporoblasts/spores	Spore shape
Anacostracospora rigaudi	unknown	Monokaryotic	Plasmotomy	32-64*	Oval
Enterocytospora artemiae	Binary fission	Monokaryotic	Plasmotomy	64-128*	Sub-spherical
Ordospora duforti	Plasmotomy from rosette	Monokaryotic	Plasmotomy	4 and 8	pyriform
Vavria anostraca	Plasmotomy	Monokaryotic	Plasmotomy	unknown	Oval
Glugoides intestinalis	Plasmotomy	Monokaryotic	Plasmotomy	16	Oblong to lightly reniform
Cystosporogenes operophterae	Binary fission	Monokaryotic	Plasmotomy	>128	Oval
Endoreticulatus schubergi	binary/multiple division	Monokaryotic	Plasmotomy	32	Oval
Crispospora chironomi	Plasmotomy by rosette	Monokaryotic	Plasmotomy	unknown	1/ sub-spherical; 2/oval
Orthosomella operophterae	Plasmotomy	Monokaryotic	Plasmotomy from sausage-shaped sporogonial plasmodium	12	Oblong to lightly reniform
Desmozoon lepeophtherii	Binary fission followed by plasmotomy	Monokaryotic	Plasmotomy	unknown	sub-spherical
Enterocytozoon bieneusi	Plasmotomy	Monokaryotic	Plasmotomy	unknown	sub-spherical to oval
Enterocytozoon hepatopenaei	unknown	Monokaryotic	Binary fission	unknown	Oval
Enterospora canceri	Plasmotomy	Monokaryotic	Plasmotomy	>20	Oval
Hepatospora eriocheir	Rosette-like division	Monokaryotic	Plasmotomy/Rosette-like division	unknown	Oval
Liebermannia covasacrae	Binary fission	Monokaryotic	Binary fission	unknown	Ovocylindrical

* Estimation from repeated observations of parasitophorous vacuoles on semi-thin sections.

Table S4. (continued)

Microsporidian species	Spore size (µm)	Spore nuclei	Spore wall thickness (nm)	Polar tube	Polar tube coils	Polar tube rows	Polar tube diameter (nm)
Anacostracospora rigaudi	1.3x0.7	Monokaryotic	55	Isofilar	5 to 6	1 to 2	60
Enterocytospora artemiae	1.2x0.9	Monokaryotic	80	Isofilar	4	1	100
Ordospora duforti	1.70x0.98	Monokaryotic	140-150	Isofilar	8 to 11	2	97
Vavria anostraca	mi:2.8-3.5x 1.5-2.0; ma: 3.5-5.0x2.0-3.0**	Monokaryotic	94x97	Anisofilar	mi: 11-12; ma: 15-18**	mi: 1; ma:2**	mi: 70-90; ma: 92-120**
Glugoides intestinalis	2.4-2.7x1.1-1.7	Monokaryotic	80-85	Isofilar	5 to 8	1	77-85
Cystosporogenes operophterae	2.7x1.6	Monokaryotic	125	Isofilar	10 to 12	1	120
Endoreticulatus schubergi	2.5x1.5	Monokaryotic	50	Isofilar	7 to 9	1	100
Crispospora chironomi	1/ 1.5-2; 2/2.5x1.5	1/ monokaryotic; 2/diplokaryotic	60	Isofilar	4	1	85
Orthosomella operophterae	3.5x1.3	Monokaryotic	50	Isofilar	6 to 7	1	75
Desmozoon lepeophtherii	2.34x1.83	Monokaryotic	75	Isofilar	5 to 8	2	65-85
Enterocytozoon bieneusi	1.5x0.8	Monokaryotic	30-35	Isofilar	4 to 7	1	75
Enterocytozoon hepatopenaei	1.1x0.7	Monokaryotic	55	Isofilar	5 to 6	2	666
Enterospora canceri	1.3x0.7	Monokaryotic	32	Isofilar	4 to 5	2	85
Hepatospora eriocheir	1.8x0.9	Monokaryotic	55	Isofilar	7 to 8	1	120
Liebermannia covasacrae	2.2-3.4x1.1-1.7	Monokaryotic	120	Isofilar	3 to 5	1	120

** mi: microspore, ma: macrospore